



HAL
open science

Influence of Sharklet-Inspired Micropatterned Polymers on Spatio-Temporal Variations of Marine Biofouling

Elora Védie, Raphaëlle Barry-Martinet, Vincent Senez, Mattias Berglin, Patrik Stenlund, Hugues Brisset, Christine Bressy, Jean-françois Briand

► **To cite this version:**

Elora Védie, Raphaëlle Barry-Martinet, Vincent Senez, Mattias Berglin, Patrik Stenlund, et al.. Influence of Sharklet-Inspired Micropatterned Polymers on Spatio-Temporal Variations of Marine Biofouling. *Macromolecular Bioscience*, 2022, 22 (11), pp.2200304. 10.1002/mabi.202200304 . hal-04304671

HAL Id: hal-04304671

<https://hal.science/hal-04304671v1>

Submitted on 24 Nov 2023

HAL is a multi-disciplinary open access archive for the deposit and dissemination of scientific research documents, whether they are published or not. The documents may come from teaching and research institutions in France or abroad, or from public or private research centers.

L'archive ouverte pluridisciplinaire **HAL**, est destinée au dépôt et à la diffusion de documents scientifiques de niveau recherche, publiés ou non, émanant des établissements d'enseignement et de recherche français ou étrangers, des laboratoires publics ou privés.

Influence of Sharklet-Inspired Micropatterned Polymers on Spatio-Temporal Variations of Marine Biofouling

Elora Védie,* Raphaëlle Barry-Martinet, Vincent Senez, Mattias Berglin, Patrik Stenlund, Hugues Brisset, Christine Bressy,* and Jean-François Briand

This article aims to show the influence of surface characteristics (microtopography, chemistry, mechanical properties) and seawater parameters on the settlement of marine micro- and macroorganisms. Polymers with nine microtopographies, three distinct mechanical properties, and wetting characteristics are immersed for one month into two contrasting coastal sites (Toulon and Kristineberg Center) and seasons (Winter and Summer). Influence of microtopography and chemistry on wetting is assessed through static contact angle and captive air bubble measurements over 3-weeks immersion in artificial seawater. Microscopic analysis, quantitative flow cytometry, metabarcoding based on the ribulose biphosphate carboxylase (*rbcL*) gene amplification, and sequencing are performed to characterize the settled microorganisms. Quantification of macrofoulers is done by evaluating the surface coverage and the type of organism. It is found that for long static in situ immersion, mechanical properties and non-evolutive wettability have no major influence on both abundance and diversity of biofouling assemblages, regardless of the type of organisms. The apparent contradiction with previous results, based on model organisms, may be due to the huge diversity of marine environments, both in terms of taxa and their size. Evolutive wetting properties with wetting switching back and forth over time have shown to strongly reduce the colonization by macrofoulers.

renewable energy devices and sensors.^[1–5] This natural and complex process corresponds to the colonization of any structures immersed in seawater by a wide diversity of marine organisms such as bacteria, diatoms, algae, or barnacles.^[1]

Many approaches to managing marine biofouling have been and are still being developed. Today, two main categories of antifouling (AF) strategies can be found: chemically active coatings and non-toxic coatings. The former use active chemicals such as biocides or enzymes, to inhibit or reduce the settlement of organisms. But this system has limitations such as durability, maintenance, toxicity, and selectivity with the release of chemicals and/or enzymatic components in water that also affects non-targeted organisms in seawater.^[6,7] Non-toxic coatings aim to reduce the settlement and/or to increase the release of settled organisms, with fouling-release (FR) coatings, superhydrophobic materials or engineered microtopographies.^[8–13] Interest in bioinspiration and biomimetic approaches for AF applications has been also the focus of much research over the past


decade. Efficient AF surfaces in nature such as marine algae combine several strategies/properties such as chemical/enzymes production and release, nano and micro-topography, association of different wetting properties of the skin or mechanical

1. Introduction

Marine biofouling directly affects the naval and offshore industries as well as desalination plants, aquaculture, marine

E. Védie, R. Barry-Martinet, H. Brisset, C. Bressy, J.-F. Briand
Laboratoire MAPIEM
E.U. 4323
SeaTech Ecole d'Ingénieur
Université de Toulon
CS 60584, Toulon 83041 Cedex 9, France
E-mail: vedie.elora@gmail.com; christine.bressy@univ-tln.fr

V. Senez
Univ. Lille
CNRS
Inserm
CHU Lille
UMR9020-U1277 – CANTHER – Cancer Heterogeneity Plasticity and Resistance to Therapies
Lille F-59000, France
M. Berglin, P. Stenlund
RISE Research Institutes of Sweden AB
Arvid Wallgrens backe 20, Göteborg SE-413 46, Sweden

 The ORCID identification number(s) for the author(s) of this article can be found under <https://doi.org/10.1002/mabi.202200304>

© 2022 The Authors. Macromolecular Bioscience published by Wiley-VCH GmbH. This is an open access article under the terms of the Creative Commons Attribution License, which permits use, distribution and reproduction in any medium, provided the original work is properly cited.

DOI: 10.1002/mabi.202200304

grooming.^[14] This suggests that developing an AF coating/system should go through the association of several of these strategies, not by focusing on a single strategy.

The settlement of marine organisms is an overly complex subject that depends on environmental variables such as pH, salinity, nutrients, flow, interactions with other organisms, temperature, etc.,^[15] but also on the properties of the immersed substrate, such as chemical composition, wettability,^[6,16] surface charges, surface free energy,^[15] surface roughness or topography,^[6,17–21] mechanical properties, like the elastic modulus.^[6]

Few studies investigated the combined effect of several parameters associated with microtopography on marine fouling and studies investigating the behavior of substrates with microtopography in a field environment are not numerous as well.^[6] In the literature, most research on microtopography investigated and showed the reduction of organism attachment on one or more microtopographies commonly associated with polydimethylsiloxane elastomer (PDMSe) or modified-PDMSe. However, bioadhesion assays were mainly performed with a single organism, usually *Ulva linza* spores or barnacle larvae.^[12,13,19] PDMSe is a material that is hydrophobic, with a low elastic modulus, which allows an easy release of many attached organisms and is also easy to process while giving an exceptionally good resolution during replication of microtopographies. Brzozowska et al. showed that material with microtopographies with higher elastic modulus such as poly(methylmethacrylate) (PMMA), lead to increased accumulation of biomass and higher adhesion (less removal through water cleaning) compared with materials with microtopographies with lower elastic modulus, such as polydimethylsiloxane (PDMS) or polyurethane (PU).^[36] It is then of interest to investigate furthermore the effect of various materials with various properties associated with one or several microtopographies.

Attachment theory describes the idea that for an organism of a given size, a microtopography that would prevent its settlement, should have protrusions with a high aspect ratio, with a significantly small surface area at the top compared to the size of the organism, with a height high enough to increase the instability in the organism's settlement. The protrusions should also be spaced of a distance slightly less than the size of the target organism, to prevent it from passing through the protrusions and settling at the base, but not too close to each other so that the organism would have difficulty to stabilize itself when trying to settle. Therefore, any microtopography tailored to one range of organism size should not be efficient against smaller organisms, that will be able to pass through the protrusion and settle at the base, nor against bigger organisms, that would encounter no issue of stability while settling.

This study presents the investigation of the effect of engineered shark skin-inspired microtopographies, applied on polymers with various properties, on marine biofouling in two contrasting field environments. The designed microtopographies were based on the Sharklet AF pattern, whose effect on colonization has been widely studied in the literature.^[18,19,22–25] In this way, the repeating unit of the pattern has the shape of a diamond.^[18,22] To target a larger variety of organisms, eight Sharklet patterns were developed. Two “basic” sharklets of different dimensions were designed and fabricated to be used as

references: 20SK and 44SK. The 20SK has 40 μm height, 20 μm width and spacing. The features are aligned such that the order of length (μm) is: 40, 80, 120, 160, 120, 80, and 40. The 44SK has 45 μm height, 44 μm width and spacing. The features are aligned such that the order of length (μm) is: 45, 180, 270, 345, 270, 180, and 45. This last specific microtopography in PDMSe has already been tested against *Amphibalanus amphitrite* cyprids in a laboratory test and showed a 97% reduction in attachment compared to smooth PDMSe.^[19] 20SK has been chosen to be part of this study as a reference with the literature. The idea was to create variation in the height of the protrusions. Three additional patterns were designed with two different heights of features within the repeating unit to create notches. For every six protrusions, the height of the protrusions was smaller than the others. Three additional designs, on their side, had a continuous variation in height to create waviness.

All these microtopographies were applied to six materials with various elastic moduli and wetting properties, in order to try to understand the relative influence of these three parameters (mechanical properties, wetting properties, and microtopographies) on the settlement of marine organisms. Immersions were performed in the Toulon Bay (France) and in the Kristineberg Center for Marine Research and Innovation (west coast of Sweden; N58.249861, E11.445194, Baltic Sea transition zone), in two seasons for the first one, to assess the influence of different environmental conditions on the antibiofouling efficacy of the substrates. Biofouling was assessed by visual characterization of the main macrofouler groups, but also in terms of bacterial and diatom densities using flow cytometry and optical microscopy. Finally, a specific determination of the composition and diversity of diatoms communities was carried out using metabarcoding.

2. Experimental Section

2.1. Materials

A PDMS (Sylgard 184 Silicone Elastomer, eSi) kit was purchased from Dow Corning and crosslinked via hydrosilylation at room temperature after degassing any bubbles under vacuum. A PU elastomer (PURA45 kit, ePU) was purchased from Reckli and crosslinked via polycondensation at room temperature. Low-density polyethylene (LDPE, Escorene LD600BA) and high-density polyethylene (HDPE, Rigidex HD6070EA) were purchased from GoodFellow. Two ester-grade thermoplastic PU, TPU AU (Desmopan 9095AU) and TPU DU (Desmopan 9885DU), were purchased from Covestro. Hempasil X3, a commercially available fouling release coating (FRC) was purchased from Hempel S.A. and crosslinked via polycondensation at room temperature. PU polymers were selected to represent hydrophilic properties for all the hardness range. LDPE and HDPE polymers were selected for the hydrophobic behavior and for a mid-hardness (100–200 MPa) and a high-hardness (1–2 GPa) material, respectively. Of all the publications reviewed by Carve et al., PDMS was investigated in 65% of the studies on the effect of microtopographies against fouling.^[12] Therefore, for the hydrophobic elastomer, PDMS (eSi) was selected for comparison with previous works with similar research interests.^[12,13,19]

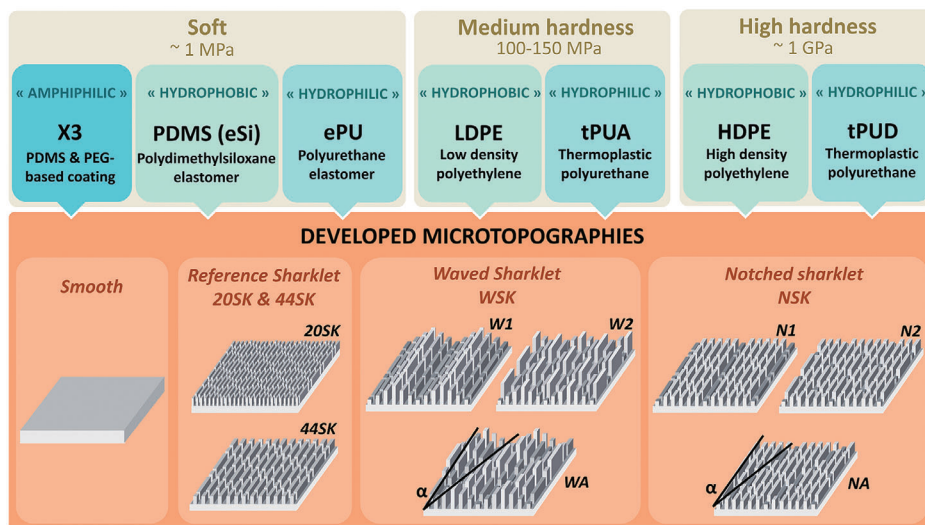


Figure 1. Summary of the selection of materials and microtopographies developed. Materials are classified in terms of wetting properties and mechanical properties.

2.2. Microtopographies

The design of the studied microtopographies were all based on the Sharklet AF pattern. Two reference one-level Sharklets, 20SK and 44SK were developed by multiplying by 10 for the 20SK pattern and by 22 for the 44SK pattern compared to the Sharklet AF pattern width and spacing features dimensions which are 4 μm -height, 2 μm -width and spacing and lengths of 4, 8, 12, 16, 12, 8, and 4 μm in the order. 20SK molds were fabricated at the Institute of Electronics, Microelectronics and Nanotechnology (IEMN, Lille, France) through the association of photolithography followed by a plasma etching.^[13] As 20SK was a pattern already investigated in a previous study,^[19] it was chosen to serve as a reference with literature. 44SK molds were fabricated at the Research Institute of Sweden (RISE, Gothenburg, Sweden), using DLP 3D printing technique.^[26–30] Notched (NSK) and waved (WSK) molds were designed based on the 44SK pattern. Three sub-categories were fabricated for both NSK and WSK features as shown in **Figure 1**. The labels N1, N2, and NA were assigned to features with a periodic variation in height and W1, W2, and WA labels were assigned to features with variable heights for each of them creating a wavy texture. A was assigned to the angle α applied to the features.

To simplify the graphics and data, a code was attributed for each polymer and microtopographies. **Table 1** summarizes the nomenclature used for microtopographies.

All the microtopographies were then transferred to the 7 materials described above through several steps using hot embossing and casting methods.^[31] The dimensions of replicated patterns on polymers were recorded using a digital microscope from 3D pictures and are summarized in Tables S1–S5 (Supporting Information). Pictures are displayed in Figure S1 (Supporting Information) for SK20 and SK44 patterns associated with all the polymers. The type of microtopographic profile for 20, 44, NSK, and WSK are schematically drawn in Figure S2 (Supporting Information). Digital microscopy images of all the microtopographies associated with PDMS (eSi) are displayed in **Figure 2**. Samples were

Table 1. Nomenclature for microtopographies.

Microtopographies	
Name	Code
Smooth	S
Sharklet 20 or 20SK	20
Sharklet 44 or 44SK	44
Notched SK 1	N1
Notched SK 2	N2
Notched SK A	NA
Waved SK 1	W1
Waved SK 2	W2
Waved SK A	WA

named as the following example: 20eSi refers to the PDMS (eSi) sample with the 20SK microtopography. SeSi refers to the smooth PDMS (eSi) sample.

For the analysis of the immersion of the different samples, the place and the season were added to the nomenclature. 20eSiTW means that the PDMS polymer with a 20SK microtopography (20) was immersed in Toulon (T) during winter (W). The letter G is used for an immersion in Kristineberg Center and S for summer.

2.3. Characterization of Substrates Properties Before Immersion

2.3.1. Mechanical Characterization

The bulk elastic modulus (E) of polymers was assessed through micro-tensile procedure using a Dynamic Mechanical Analyser (Q800 DMA, TA Instruments) using the tension film clamp along with the DMA strain rate mode. Rectangular-shaped triplicates were cut out from smooth samples of every material. As the Q800

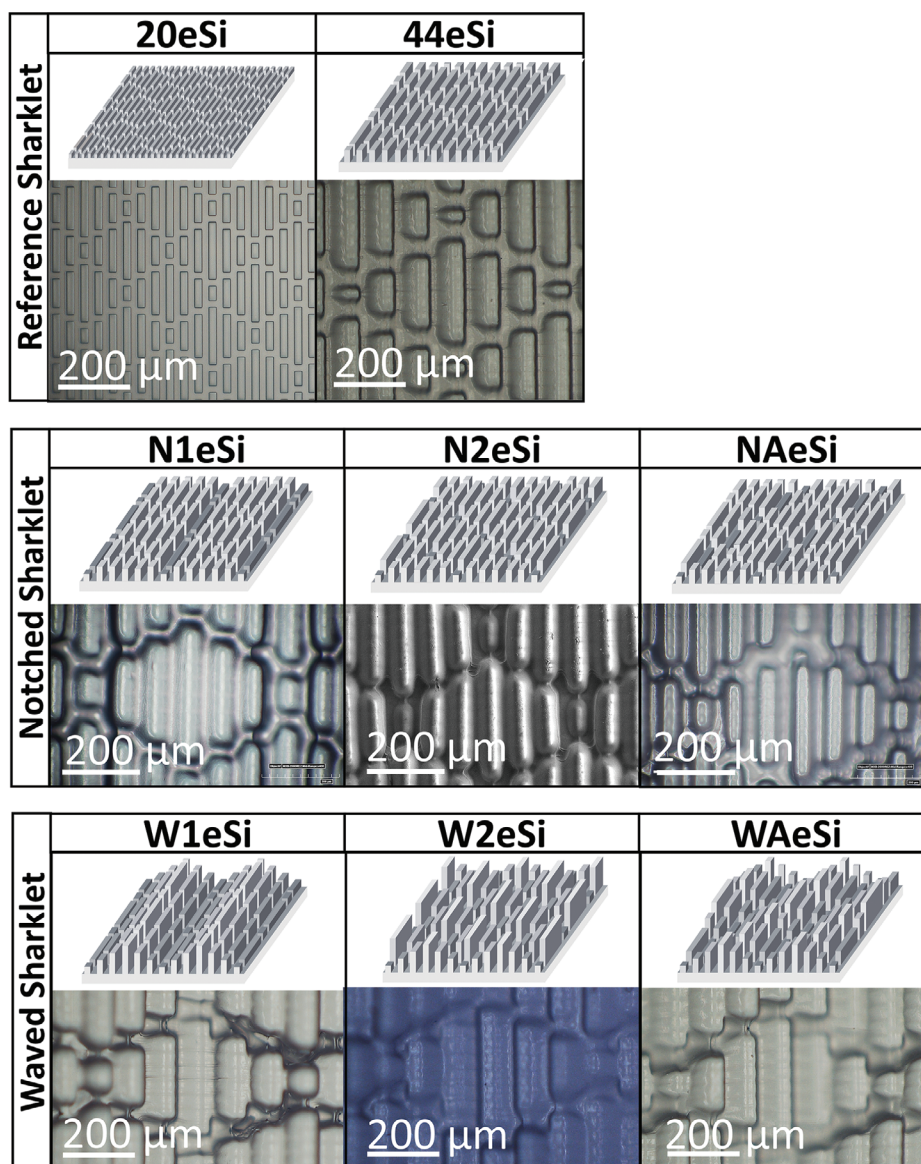


Figure 2. Illustration and digital microscopy image of all the developed microtopographies applied on PDMS elastomer (eSi) to illustrate the obtained substrates after replication.

DMA cannot exceed 18 N of static force, the surface area of some samples such as HDPE and tPUD had to be adjusted to this limit, to evaluate their elastic modulus. The dimensions of the samples were around 5 mm in length between the clamps, 2 mm in width, and 1 mm thick, for HDPE and tPUD the width and length were adjusted depending on the thickness of the substrates. After a preload of 0.001 N, that prevents loose attaches, samples were stretched. Elastic modulus values were taken from the slope of the stress-strain curves in the elastic domain.

2.3.2. Wetting Properties

Static contact angle values (SCA) with a 2 μ L-ultrapure water droplet were assessed in air environment. The surface free

energy γ_s and its dispersive γ_s^d and polar γ_s^p components of all polymers were assessed by the Owens and Wendt method through the measurements of static contact angle using two polar liquids, water (w) and glycerol (g) and one less polar liquid, diodomethane (d). Wetting behavior of substrates, when immersed in seawater, was investigated throughout static captive air bubble measurements (SCB) in artificial seawater (ASW) with a salinity of 36 g L⁻¹.^[32] Due to the anisotropic pattern of the studied sharklet, all the contact angle measurements were performed in two directions, i.e., parallel to features (\parallel) and perpendicular to features (\perp). For example, samples were named 20eSi \parallel and 20eSi \perp which refer to PDMS (eSi) samples with the 20SK microtopography, \parallel refers to an image capture when camera is pointed toward the droplet and its direction of spreading is parallel to the features and \perp refers to an image capture with the camera point-

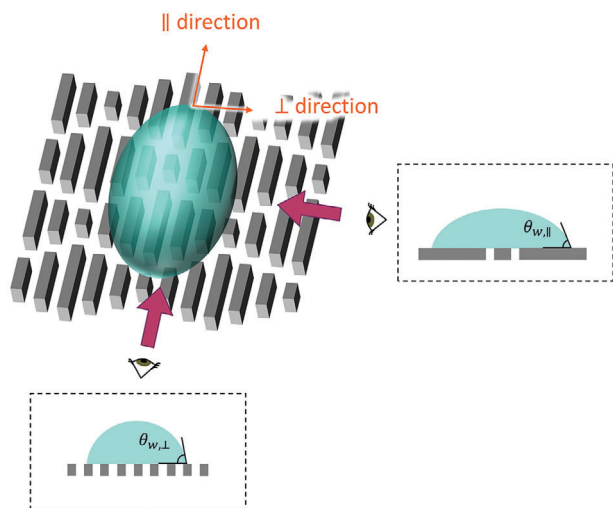


Figure 3. Illustration of the angles of observation used for each sharklet-based sample. \perp refers to an image capture with the camera pointing to the droplet when its direction of spreading is perpendicular to the features and \parallel refers to an image capture when camera is pointed toward the droplet and its direction of spreading is parallel to the features.

ing to the droplet when its direction of spreading is perpendicular to the features (**Figure 3**).

2.4. Immersion of the Substrates in Marine Environment

2.4.1. Field Immersion Periods

Samples were deployed in static field immersion tests in two different seasons: one in winter and two in summer. The winter static field immersion test was carried out in the Toulon Bay (North-western Mediterranean Sea). All smooth, 20SK, N1, N2 and NA patterned substrates were tested in four replicates. A one-month immersion, from 2019, November 12th to 2019, December 9th-10th, was carried out for microfouling investigations. Three replicates were used for analyses. The last replicate was used for longer immersion time (up to 211 days) to assess its efficiency against macrofouling over time. eSi, ePU, X3, HDPE, LDPE, tPUA, and tPUD were investigated.

Based on the available 44SK and WSK micropatterned molds from Sweden and the results obtained from the first campaign of immersion in Toulon, all smooth, 44SK, W1 and WA patterned substrates were tested in four replicates during the summer season. Three replicates were used for microfouling analyses after a one-month immersion in both the Toulon Bay, France and the Kristineberg Center, Sweden. The Kristineberg Center and the Toulon Bay are two contrasting environments in terms of bio-foulers. The Kristineberg Center is known, in summer, for its large abundance of barnacles, which are the predominant macro-foulers in this site. Barnacles are the hard foulers the most impacting and destructive regarding marine industry, being one of the main reasons of ship's hydrodynamic decrease. Thus, barnacle settlement has been largely studied in lab experiments. As these organisms are not generally abundant in the bay of Toulon, it appears relevant to immerse panels in this site to provide the opportunity to investigate barnacles' settlement in an in situ en-

vironment and to get diversified fouling assemblages. The two summer immersions lasted one month, from July 23rd, 2020, to August 25th, 2020 for the immersion in France, and from August 12th, 2020, to September 14th, 2020 for the immersion in Sweden. In both sites, the samples were immersed at the same depth of 1 m. The last replicate was meant to stay for one year, to see the evolution of macrofouling over time in Toulon. Only eSi, ePU, X3, HDPE, and tPUD were investigated for this second campaign.

A nomenclature was set for samples immersed in natural sweater. 20eSiTW means that the eSi polymer with a 20SK micropography (20) was immersed in Toulon (T) during winter (W). The letter G is used for an immersion in Kristineberg Center and S for summer, i.e., 20eSiGS.

2.4.2. Supports for Field Immersion Tests

The substrates were mounted on poly(vinylchloride) (PVC) plates of 36 cm \times 18 cm. A plastic sheet with holes cut in a square pattern was placed on top of all substrates, to make sure that the same area (5 cm \times 5 cm) of each substrate was exposed to the marine environment. The whole was maintained with PVC pieces screwed with polyamide screws (**Figure S3**, Supporting Information). The panels were submerged at a depth of \approx 1 m.

2.4.3. Environmental Parameters Measurements

At Toulon, water temperature, pH, salinity, and dissolved oxygen were measured using a Hydrolab DS5X probe (Hatch Hydromet, USA) at t_0 , $t_{15\text{days}}$ and t_{end} . Nutrients (NO_3^- , PO_4^{3-} , $\text{Si}(\text{OH})_4$) were also analyzed using standard colorimetric methods for seawater.^[33] At Kristineberg Center, temperature, salinity, and pH were measured every 15 min during the immersion period.

2.5. Characterization of Fouling Communities

2.5.1. N Quantification

The AF efficiency (N) was assessed over immersion time in static conditions. Percentage of macrofouling communities such as algae (brown, green, red), hydrozoans, spirorbid worms, bryozoans, tubeworms, barnacles, and colonial ascidians settled on the substrates were recorded following the updated NF-T-34-552 standard which describes the practice for evaluating the AF efficiency of chemically active AF coatings.^[34] Panels were inspected without rinsing the substrates.

In this standard procedure, the percentage of surface covered by marine organisms (intensity factor, IF) and the type of fouling organisms (severity factor, SF) are recorded (**Table 2**). AF coatings are classified using an efficiency parameter N, which is expressed as:

$$N = \Sigma (IF \times SF) \quad (1)$$

For the best AF behavior, N equals 5 (on the assumption there is always some biofilm on the immersed panel) and for the worst, N is usually close to 40 (maximum of coverage with several types of macrofoulers).^[32]

Table 2. Evaluation of the efficiency parameter N. Adapted from.^[34]

Fouling coverage		Type of fouling	
% coverage	Intensity Factor IF	Fouling Type	Severity Factor SF
No fouling	0	Biofilm	1
0 ≤ % ≤ 10	1	Algae (brown, red, green)	3
10 < % ≤ 20	2	Non-encrusting species (Hydrozoa, sponges, ascidians, ...)	4
20 < % ≤ 40	3	Encrusting species (Barnacles, tubeworms, spirorbid worms, bryozoans, shells,...)	6
40 < % ≤ 60	4		
60 < % ≤ 100	5		

2.5.2. Sampling Strategy and Method for Microfouling Assessment

For each combination microtopography/material, three replicates were fabricated. The three replicates were divided in three zones of 1.6 cm × 5 cm, one for diatom microscopic analysis and one for bacterial density determination using flow cytometry. The last zone of each sample was dedicated to deoxyribonucleic acid (DNA) analysis on sample 1, to Low Vacuum-Scanning electron microscopy (LV-SEM) on sample 2 and was discarded on sample 3 (Figure S4, Supporting Information). Except for SEM, biofouling was collected on each zone by scraping the surfaces with a sterile scalpel.

2.5.3. Diatom Microscopic Analysis

The collected biofouling was fixed in 10 mL of 0.3% lugol-sterile ASW solution (with a 36 g L⁻¹ sea salts concentration) and refrigerated at 4 °C in the dark between analyses. Cell numeration was performed under a light microscope (1000× magnification, at least 30 fields or 100 cells). Biovolumes were calculated to better estimate surface coverage of the samples.^[35]

2.5.4. Quantitative Flow Cytometry Analyses

Flow cytometry analyses were performed to investigate the density of heterotrophic prokaryotes on the surface of each micropatterned substrate. Only smooth materials were analyzed for the winter immersion in the Toulon Bay. The collected biological material was fixed in 4 mL of 0.25% glutaraldehyde-sterile artificial seawater (ASW) solution (with a 36 g L⁻¹ sea salts concentration), carried in a cooler from the immersion site to the laboratory and stored at -80 °C between the collection and the analysis. Before the analysis, 4 μL of Tween 80, 800 μL of sodium pyrophosphate (PPiNa) at 10 mM and 3.2 mL of ASW (with salinity of 36 g L⁻¹) were added to each collection tube. Aggregate cells were dissociated with a 3 min sonification. After 15 min in ice, the tubes were vortexed and centrifugated for 1 min at 800 g. The supernatant was filtered using EASYstrainer cell sieves of 40 μm.^[36] The obtained solution was then diluted to the tenth and SYBR green was added to stain the heterotrophic prokaryotes. Heterotrophic prokaryotes were numbered using a BD Accuri C6 flow cytometer (BD Biosciences, San Jose, CA, United States) at the Regional

Flow Cytometry Platform for Microbiology (PRECYM). Data were acquired using BD Accuri Cflow Plus software. Results were expressed as a density of cells per cm².

2.5.5. DNA Extraction, RbcL Gene Amplification and Sequencing

DNA was extracted from scratched material using the Dneasy PowerBiofilm Kit (Qiagen). rbcL gene amplification was performed by polymerase chain reaction (PCR), using equimolar primers mix (described by Vasselon and colleagues).^[37] PCR program was the following: 95 °C-15', 95 °C-45", 55 °C-45", 75 °C-45", 75 °C-5'. Step 2 to 5 were performed during 40 cycles.

Amplicons were then paired end sequenced (2 × 300 bp) on an Illumina platform (Eurofins Genomics, Konstanz, Germany). Two samples did not achieve any read (WaeSiGS and WAT-PUDGS) and will not be part of metabarcoding analysis.

2.5.6. Low Vacuum Scanning Electron Microscopy (LV-SEM)

LV-SEM of fresh samples was performed with a TM 4000 (Hitachi, IHU Marseille) under low vacuum (30 Pa) (working distance between 5.7 and 9.6 mm, accelerating voltage: 10–15 kV).

2.5.7. Data Processing

Raw sequences were cleaned and filtered with FROGS.^[38] Clustering relies on Swarm which does not agglomerate sequences based on the typical 97% threshold but relies instead on both the number of differences and the likely series of accumulation of those differences.^[39] Chimera detection relies on VSEARCH with de novo UCHIME method.^[40,41] The innovative cross-sample validation step from FROGS was used to confirm the chimeric status on all samples. Rare OTUs representing less than 0.005% of all sequences were removed. Taxonomic affiliation was made on Rsyst_Diatom_7 database.^[42]

2.6. Statistical Analysis

After the measurements of SCA and SCB, ANOVA tests followed by Tukey's post-hoc tests were performed to test differences between metrics using XLSTATv7. Differences in the contact angle

Table 3. Static contact angle θ_w , θ_g , θ_d , surface free energy γ_s and its dispersive and polar components of smooth substrates. The letters a, b, c, d, e, f, and g indicate groups that are significantly different from each other (ANOVA followed by post-hoc Tukey's tests).

Polymer	$\theta_{\text{air(ASW)0}}$ [°]	θ_w [°]	θ_g [°]	θ_d [°]	γ_s [mJ m ⁻²]	γ_s^d [mJ m ⁻²]	γ_s^p [mJ m ⁻²]	E [MPa]
SeSi	36.4 ± 2.0	a 116.5 ± 0.4	b 114.8 ± 0.3	b 74.3 ± 5	22 ± 3	22 ± 3	0.0 ± 0.6	1.3 ± 0.3
StPUA	101.5 ± 2.7	b 108.7 ± 0.3	a 97.0 ± 1.0	a 72 ± 2.0	22 ± 3	22 ± 2	0.0 ± 0.2	103 ± 5
SHDPE	80.8 ± 3.9	c 99.7 ± 0.4	a 93.2 ± 0.6	c 57 ± 1.0	26 ± 9	25 ± 8	0.4 ± 0.8	1150 ± 34
SLDPE	79.9 ± 5.5	d 96.8 ± 0.5	a 94 ± 4	a 72 ± 5	21 ± 8	20 ± 6	1.0 ± 1.9	160 ± 63
StPUD	73.4 ± 2.9	e 91 ± 2	c 84.3 ± 0.6	c 58 ± 3	29 ± 6	28 ± 4	1.1 ± 1.5	1000 ± 120
SePU	55.3 ± 6.7	f 84 ± 1	c 79 ± 7	d 31.6 ± 0.6	44 ± 2	42 ± 1	1.9 ± 0.7	1.2 ± 0.2
SX3	50.6 ± 4.1	g 25.4 ± 0.5	d 55.7 ± 0.6	e 25 ± 0.4	58 ± 26	34 ± 9	24.3 ± 17.8	0.7 ± 0.2
Pr > F	NA	<0.0001	<0.0001	<0.0001	NA	NA	NA	NA
Signifi-cant		Yes	Yes	Yes				

values were evaluated between smooth and micropatterned substrates. Values with $p < 0.05$ or 0.001 or 0.0001 were considered significant. Values with $p > 0.05$ were considered as similar.

ANOVA were performed with Xlstat software to test differences for bacterial and diatom abundances, and to test differences for wetting properties. Alpha diversity indexes (Chao1, Shannon, and Inverse Simpson) and multivariate analysis of variance (with adonis, considering texturation or surface chemistry as factors, with 9999 permutations) were obtained with FROGS. One-way analysis of variance (one way ANOVA) was calculated with Xlstat software, as Non-metric MultiDimensional Scaling (NMDS), based on Bray–Curtis dissimilarity matrix for taxonomic relative abundance (obtained with FROGS). Biomarkers were highlighted with Linear Discriminant Analysis (LDA) to estimate the effect size (LefSe)^[43] of each differentially abundant feature, with FROGS, using a 5% alpha value for the factorial Kruskal–Wallis test and a threshold of 4.5 on the logarithmic LDA score. Analyses were performed considering Site or Season as classes and substrates as subclasses.

3. Results

3.1. Mechanical Properties of Smooth Polymer Films

Polymers were selected for their wide range of elastic moduli from MPa to GPa, with elastomeric to thermoplastic behavior. In the elastomer range, eSi and ePU showed similar elastic modulus around 1 MPa and X3 showed the smallest elastic modulus with 0.7 ± 0.2 MPa. The two thermoplastics, LDPE and tPUA, showed an elastic modulus of 160 ± 63 and 103 ± 5 MPa, respectively. Finally, HDPE and tPUD showed an elastic modulus above 1 GPa, with 1150 ± 34 and 1000 ± 120 MPa, respectively. (Table 3)

3.2. Wetting Properties of Smooth and Micropatterned Polymer Films

3.2.1. Wetting of the Smooth Polymers

γ_s is the surface free energy available for competing with the surface tension of liquids. A higher value of γ_s transcribes surfaces that

are more easily wettable than surfaces with a low γ_s . Therefore, X3 is by far the most easily wettable substrate, which is consistent with the measured small θ_w ($25.4 \pm 0.5^\circ$). ePU showed a $\gamma_s = 44 \pm 2$ mJ m⁻² with a polar component of 1.9 ± 0.7 . HDPE and tPUD showed similar γ_s values ($\gamma_s \sim 27\text{--}30$ mJ m⁻²) and are expected to be less easily wettable than X3 and ePU. The γ_s value of HDPE was consistent with values found in the literature.^[44] eSi, LDPE and tPUA showed similar γ_s values (close to 20 mJ m⁻²), which were the lowest, making those substrates the least easily wettable substrates of all the polymers investigated. These polymers exhibit only dispersive forces at the surface. The γ_s value obtained for eSi was consistent with values found in the literature.^[45,46]

When the purpose of the surface being analyzed is to be immersed in a liquid medium, like in marine antifouling studies, it is preferable to complete the wetting characterization, with captive air bubble measurements. In this case, the substrate is immersed in the liquid in which it is intended to be immersed in.^[47] Characterizing the wetting properties in air alone will not provide sufficient detail about the surface properties, as its behavior may change when immersed through rearrangement or interaction with surrounding liquids.

It may also be useful to monitor the kinetics of any surface changes as a function of immersion time. Thus, smooth substrates were immersed for three weeks in ASW with a salt concentration of 36 g L⁻¹. This salinity was selected as it is close to the salinity found in the Mediterranean Sea immersion site.

Figure 4 shows that tPUA appears as the most hydrophobic of all substrates with a $\theta_{\text{air(ASW)0}}$ of $102^\circ \pm 2^\circ$ at t_0 . LDPE and HDPE follow in the scale of hydrophobicity and are similar at t_0 with a $\theta_{\text{air(ASW)0}}$ value of 81° and 82° , respectively ($p > 0.05$). The surface properties of X3 and ePU appear similar to each other with contact angles of 52° and 56° ($p > 0.05$), respectively, showing more hydrophilicity, as expected since they were the more hydrophilic substrates when measuring θ_w values in air.

Except for eSi and X3, the same trends are observed for $\theta_{\text{air(ASW)0}}$ at t_0 as for the static θ_w . $\theta_{\text{air(ASW)0}}$ values are 7 to 17° lower than θ_w for the more hydrophobic polymers such as tPUA, LDPE, HDPE and tPUD, while they are 30° lower for the more hydrophilic ePU. A $\theta_{\text{air(ASW)0}}$ value higher than θ_w was observed for the highly hydrophilic X3.

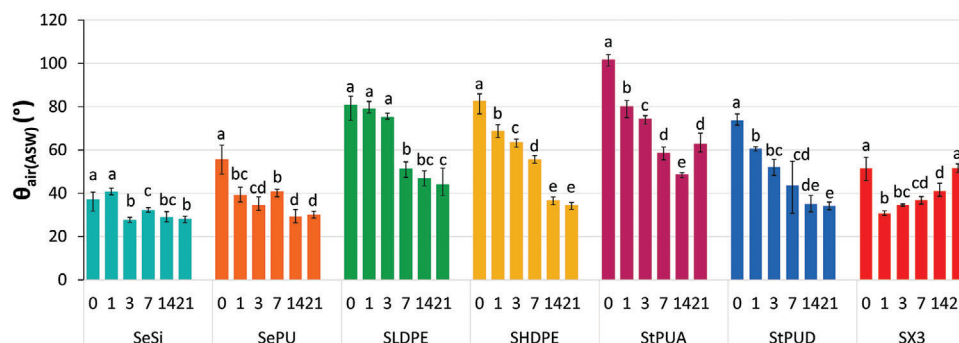


Figure 4. Evolution of the static captive bubble contact angle ($\theta_{\text{air(ASW)}}$) with immersion time for all smooth substrates, measured before immersion, and on days 1, 3, 7, 14 and 21, in ASW at a salt concentration of 36 g L^{-1} . The letters a, b, c, d, and e show similarity of $\theta_{\text{air(ASW)}}$ through a Tukey's test ($p > 0.05$).

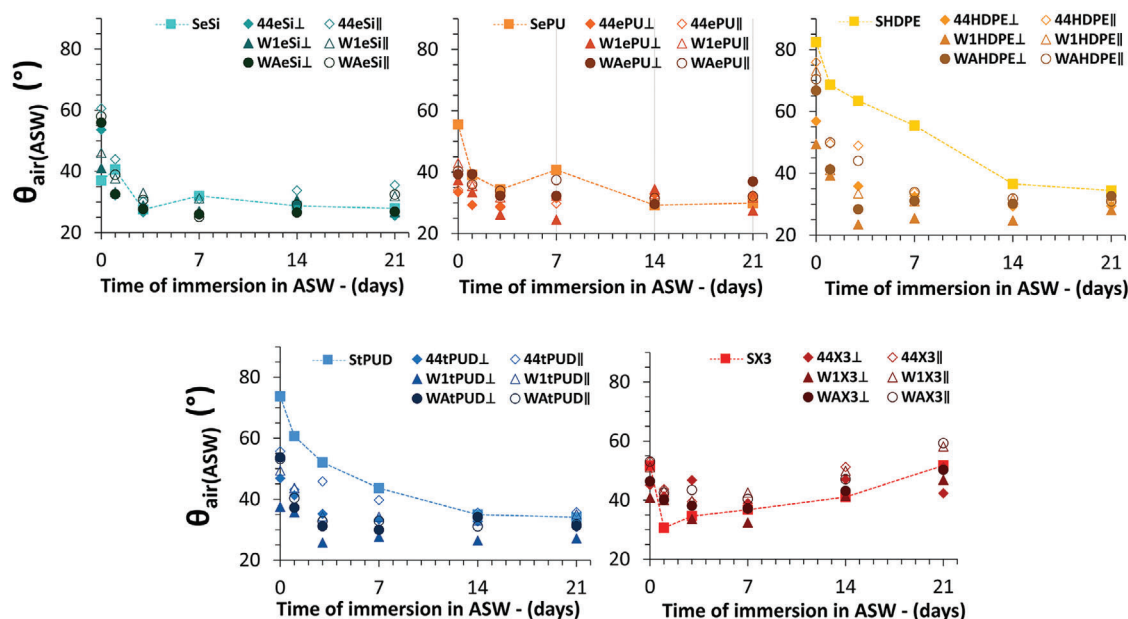


Figure 5. Static captive air bubble contact angle on smooth and micropatterned polymers over immersion time in ASW.

In addition, Figure 4 shows that $\theta_{\text{air(ASW)}}$ decreases with immersion time in ASW for most polymers. The $\Delta\theta_{\text{air(ASW)}}$ between t_0 and $t_{3 \text{ weeks}}$ dropped of 39° for tPUA, 37° for LDPE, 48° for HDPE, 40° for tPUD, 26° for ePU and 9° for PDMS. The behavior of X3 is different from the other polymers with after a drop of 21° during the first 24 h, $\theta_{\text{air(ASW)}}$ slightly increased over the 3 weeks of immersion to return to an angle similar to its initial $\theta_{\text{air(ASW)}}$ measured at t_0 .

3.2.2. Wetting of the Micropatterned Polymers Immersed in ASW

At t_0 , micropatterns influenced the wetting for all polymers. At t_0 , $\theta_{\text{air(ASW)}}$ is affected by the micropatterning showing greater hydrophilicity than their respective smooth substrates for ePU, tPUA, and tPUD (except N2tPUD||) (Figure 5; Figures S5 and S6, Supporting Information). On contrary, micropatterned eSi substrate exhibited a higher $\theta_{\text{air(ASW)}}$ than for the smooth one sug-

gesting a less hydrophilic surface than the smooth one. This result was more pronounced in the || direction than in the \perp direction. LDPE and HDPE showed a similar behavior showing lightly more hydrophilicity in the \perp direction compared to their respective smooth substrates while for the || direction they showed similar behavior than the smooth ones. 20SK microtopography showed similar behavior than other microtopographies in captive air bubble experiments except for LDPE and HDPE, where 20SK showed much more hydrophilicity compared to the other microtopographies.

To see if the effect of microtopography on wetting lasted while the substrate was immersed over a long period of time, a monitoring of the wetting of substrates immersed in ASW for 3 weeks was pursued. The experiment was only conducted on smooth, 44SK, W1 and WA microtopographies and for 5 polymers: PDMS, ePU, HDPE, tPUD, and X3. These samples correspond to the substrates that were immersed during the second campaign of immersion in summer 2020.

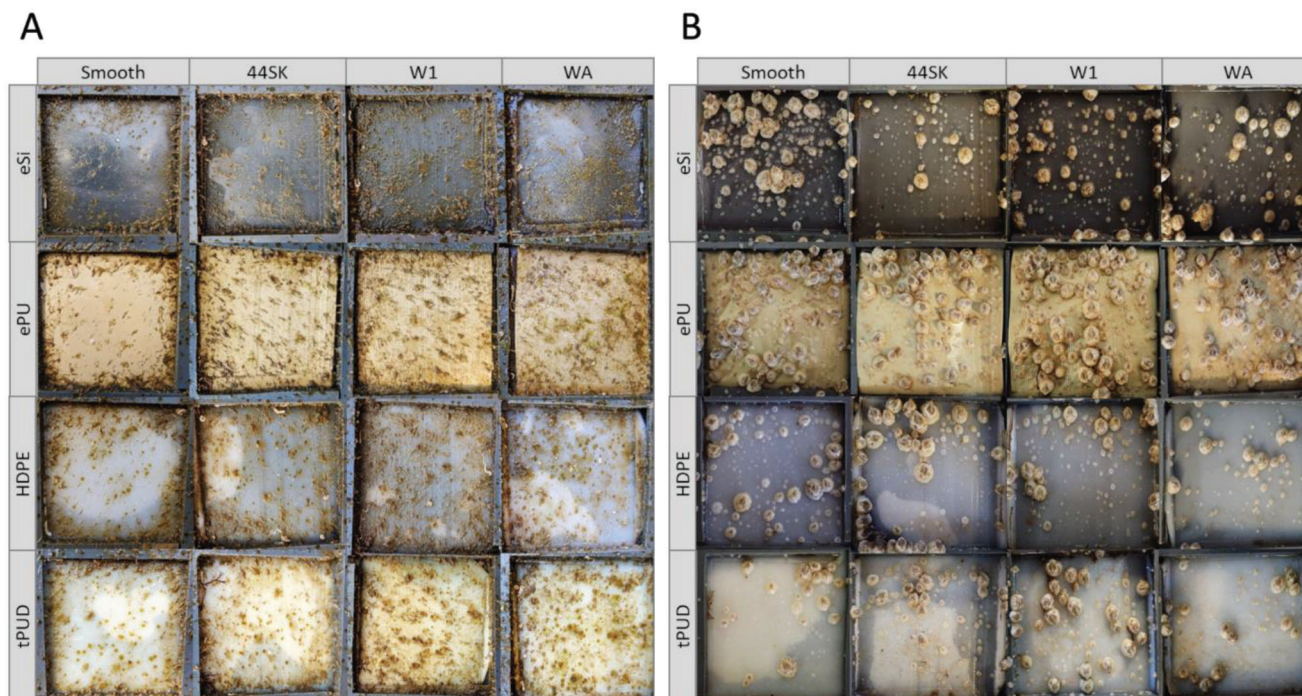


Figure 6. Photographs of substrates after one month of immersion. A) in Toulon Bay, from 2020, July 23rd to 2020, August 25th. B) in Kristineberg Center, from 2020, August 12th to 2020, September 14th.

Over time of immersion, the patterned substrates followed the same pattern of increasing hydrophilicity with immersion time as for smooth substrates but showing more hydrophilic behavior with lower values of $\theta_{\text{air(ASW)}}$ than the smooth substrates for all polymers except X3 (Figure 5). Moreover, the difference between the $\theta_{\text{air(ASW)}}$ of smooth PDMS, HDPE and tPUD compared to the $\theta_{\text{air(ASW)}}$ of the patterned polymers, tended to decrease over immersion time, meaning that the behavior of the patterned HDPE and tPUD tended to resemble the behavior of the smooth substrates after 3 weeks of immersion in ASW. Stabilization of $\theta_{\text{air(ASW)}}$ is observed over immersion time and seems to be quicker for micropatterned polymers than for smooth ones. For patterned substrates, stabilization of the $\theta_{\text{air(ASW)}}$ occurred after around 3 days of immersion. X3 was the only polymer that did not show a clear stabilization of $\theta_{\text{air(ASW)}}$. Convergence of the wetting property of smooth and patterned polymer seemed to occur, difference between smooth and patterned decreasing over time of immersion. Therefore, if any difference in colonization between patterned substrates and its smooth homolog is to be noticed after field immersion, it could be most likely attributed to an effect of the steric hindrance.

Overall, all $\theta_{\text{air(ASW)}}$ values in the \parallel direction for the patterned substrates were higher than $\theta_{\text{air(ASW)}}$ values in the \perp direction, for all polymers and all microtopographies. A higher difference between the \perp and \parallel directions was observed for immersed HDPE and tPUD and was higher than the difference between \perp and \parallel directions observed for eSi, ePU, and X3. The highest difference between \perp and \parallel directions was seen 3 days after immersion.

3.3. Evaluation of the Efficiency of Polymer Substrates Against Macrofouling

Figure 6 shows some images of samples immersed in two different sites with a contrasting macrofouling diversity and seawater parameters. Diverse groups of macrofoulers were found in the two sites. In winter, at Toulon, brown algae were the only type of macrofouling observed on the substrates. In summer, the colonization in Kristineberg Center was characterized by the presence of barnacles only, while in Toulon, the colonization was represented by heterogeneous assemblages of macrofoulers including algae (brown, green, and others), non-encrusting organisms (hydrozoans), encrusting organisms (tubeworms, *Spirorbis*) and other hard fouling such as barnacles (Figure 7B,C). Temperatures were similar at the two sites during the summer immersion whereas they were lower during the winter immersion at Toulon (Table S6, Supporting Information). A clear difference in salinity could be noticed with lower values in Kristineberg Center than in Toulon (18.0 ± 3.4 vs 38.1 ± 0.6 g L⁻¹, respectively). Nutrients measured only in Toulon exhibited significantly higher concentrations for nitrates and silicates during winter when phosphates remained similar.

Based on the coverage percentage of several groups of macrofoulers observed on these images, the efficacy parameter (N) was evaluated. In Toulon, after one month of immersion in winter, the well-known efficient X3 substrate^[48] had an efficacy parameter N of 5 whatever the microtopography, which corresponds to a high AF efficacy. After one month in summer, only the W1 \times 3 substrate had a N value higher than 5 ($N = 9$) (Figure 7A). X3 showed values statistically lower than the rest of

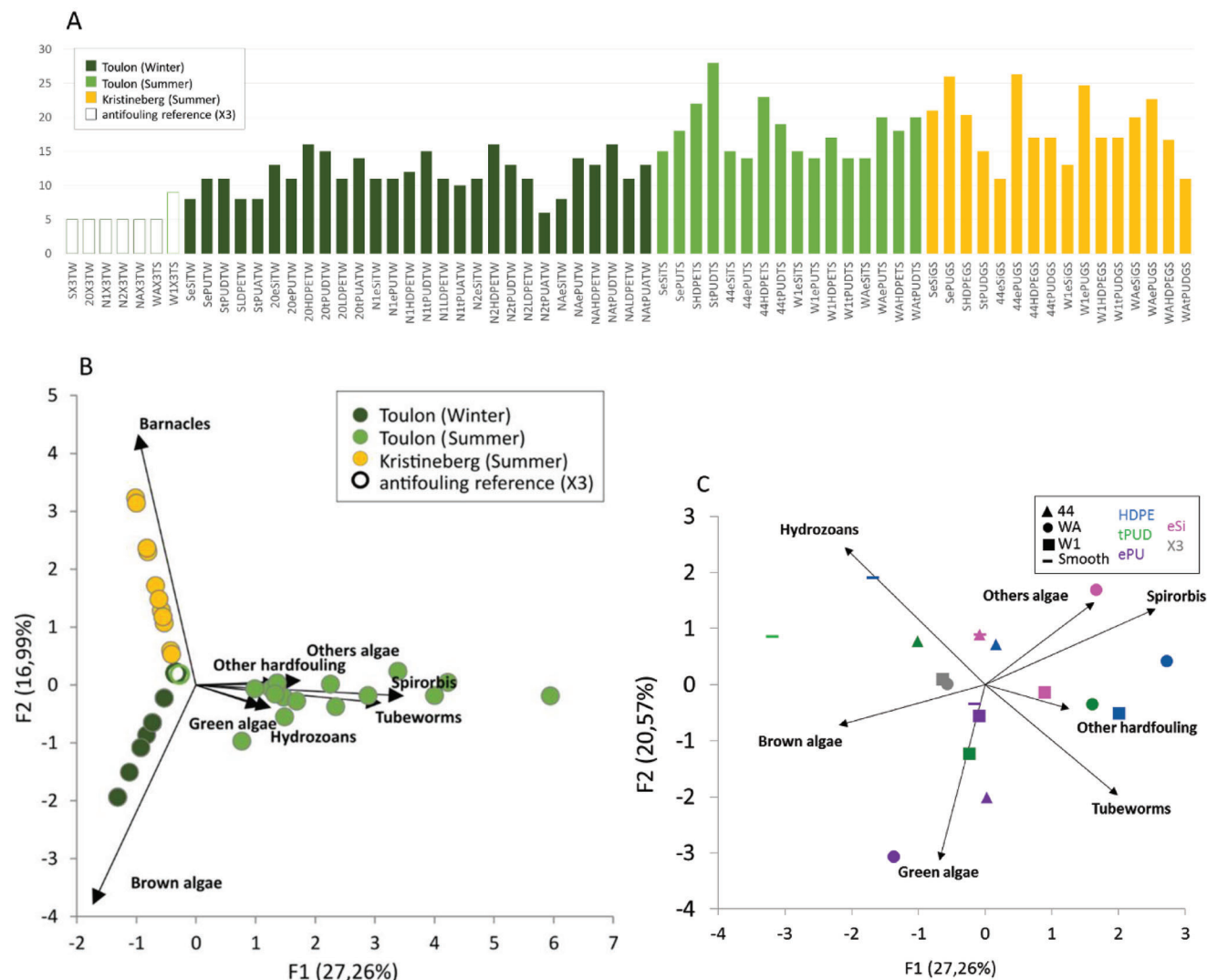


Figure 7. A) Efficacy parameter of each substrate and B) Principal Component Analysis (PCA), based on the percentage of coverage of the main groups of macrofoulers visually observed in Kristineberg Center and Toulon, with C) a focus on the summer season at Toulon.

the substrates immersed in Toulon in both seasons. During the summer campaign, SX3TS, W2 × 3TS samples were lost during the first month of immersion which is why the N values of those samples are not indicated. Only one W1 × 3TS and one WAX3TS was found after one-month immersion, as the second replicates were lost during the first month of immersion. It was chosen to analyze the microfouling on these two X3 substrates left, rather than letting them immerse to investigate the evolution of the N over time of immersion. The other substrates immersed in Toulon were characterized by an N value, which is higher in summer than in winter ($p < 0.0001$). Indeed, in winter, N started at a minimum of 6 (for N2tPUA) and reached a maximum of 16 (for 20HDPE, N2HDPE, and NatPUD), whereas it ranged from 14 (for 44ePU, W1ePU, W1tPUD, and WAesi) to 23 (for 44HDPE) in summer. In Kristineberg Center, N values were not significantly different from those in Toulon. A minimum of N = 11 was observed on 44eSi and WAHDPE, and the maximum (26) was observed on SePU and 44ePU. When looking at the

disposition of the barnacles on the substrates (Figure 6B), those seemed to settle lined up in vertical straight lines most likely following the channels created by the Sharklet (|| direction) especially for 44SK and W1 microtopographies. On WA microtopography, the barnacles seem to settle lined up in the || direction but also in the α direction (artificial channels created thanks to the variation of height in the Sharklet, Figure 2). If some influence of microtopography can be noted in the preferential settlement of the barnacles, regarding the N value which translates the covered surface percentage in this case for those fouling species, the microtopography alone did not seem to influence the total degree of settling. Indeed, when comparing all polymers (eSi, ePU, HDPE, tPUD) associated with one microtopography and their smooth homolog, there were not similar variations (for example a decrease of N for all polymers) but rather some with N increasing, and some with N decreasing. That implies that the microtopography did not drive the settlement density.

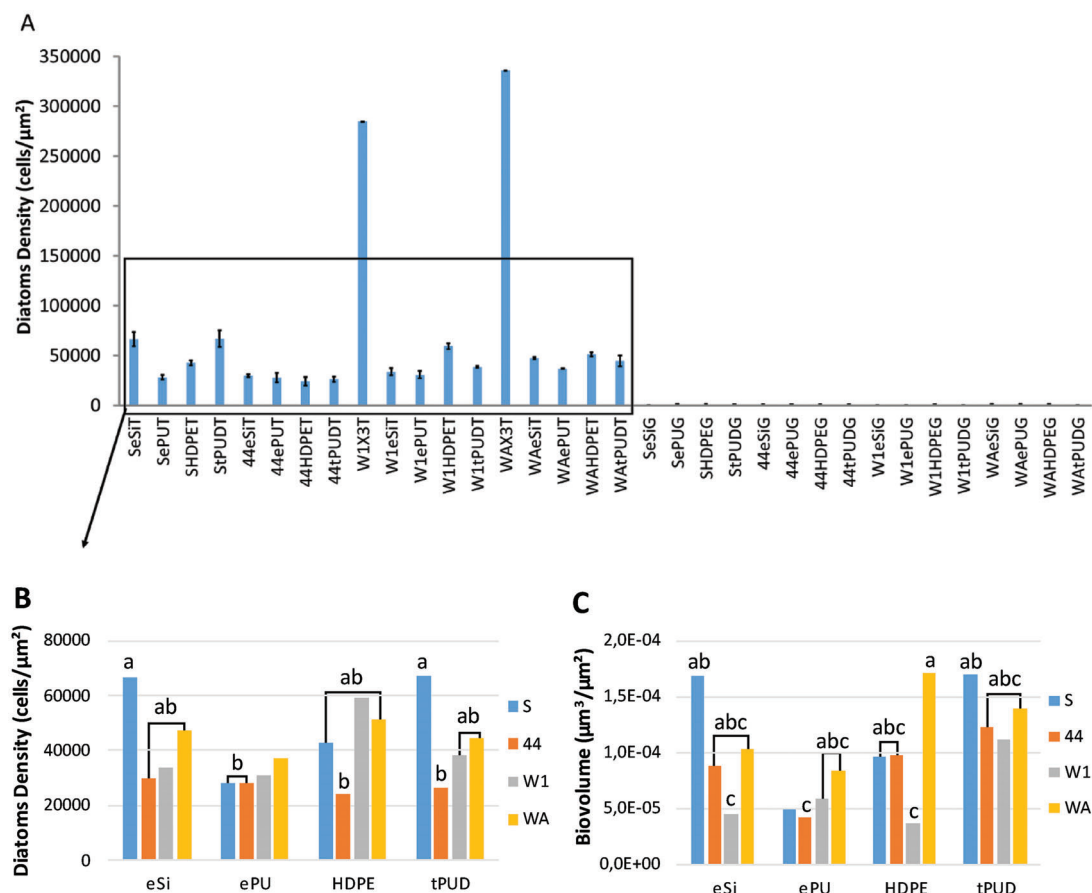


Figure 8. A) Diatom density in Toulon (T) and Kristineberg Center (G) in summer (S). B) Zoom on diatoms density and C) on biovolumes in Toulon, on eSi, ePU, HDPE, and tPUD substrates in summer.

Moreover, the PCA performed on visual inspections in Toulon in summer did not show any clustering based on the microtopography or surface chemistry (Figure 7C). Clusters are mainly site and season dependent.

In Toulon, the efficacy parameter *N* was observed until 211 days (following the winter immersion) and 254 days (following the summer immersion) (Figure S7, Supporting Information). Among remaining samples, SX3TW and N1eSiTW showed the lowest *N* value (11) in winter. All other micropatterned X3 substrates showed significantly lower efficacy than the smooth ones but X3 was still the more efficient among all other smooth and micropatterned materials (Table S7, Supporting Information). In summer, the smallest values of *N* were observed on SeSiTS (15), W1eSiTS (20), and WAeSiTS (18).

3.4. Evaluation of the Efficiency Against Microfouling

3.4.1. Bacterial Density

Considering the winter immersion in Toulon, only smooth surfaces were analyzed. Bacterial densities were significantly higher on ePU and X3 compared to the others, reaching $6.5 \cdot 10^{-4}$ and $3.1 \cdot 10^{-4}$ cells per cm^2 , respectively (Figure S8A, Supporting Information).

Considering the summer immersion, bacterial densities were overall significantly lower at Toulon compared to Kristineberg Center ($p < 0.0001$). At Toulon, WAePU, WAHDPE, and WAtPUD exhibited significant lowest densities, in the range between $7.3 \cdot 10^{-3}$ and $8.2 \cdot 10^{-3}$ cells per cm^2 ($p < 0.005$, Figure S8B, Supporting Information). At Kristineberg Center, the lowest densities were noticed for 44ePU, 44HDPE, 44tPUD, and W1ePU, in the range between $1.8 \cdot 10^{-2}$ and $2.5 \cdot 10^{-2}$ cells per cm^2 ($p < 0.005$). Figure S8 (Supporting Information) clearly demonstrates that the bacterial density is site- and season-dependent.

3.4.2. Diatom Density and Biovolume

The density of diatoms found on panels immersed in Kristineberg Center in summer did not exceed $1.0 \cdot 10^3$ cells per μm^2 whereas values from $2.4 \cdot 10^4$ to $3.4 \cdot 10^5$ cells per μm^2 were reached in Toulon (Figure 8A). W1 × 3TS and WAX3TS (Figure S10, Supporting Information) were significantly colonized by more diatoms ($2.8 \cdot 10^5 \pm 25$ and $3.4 \cdot 10^5 \pm 8$ cells per μm^2) but were the less covered substrates considering biovolume of diatoms ($1 \cdot 10^{-4}$ and $1.4 \cdot 10^{-4}$ μm^3 per μm^3 , respectively) (Figure 8C). Furthermore, substrates immersed in winter in Toulon did not show any significant differences between density or biovolumes (Figure S11A,B; Table S8, Supporting Information).

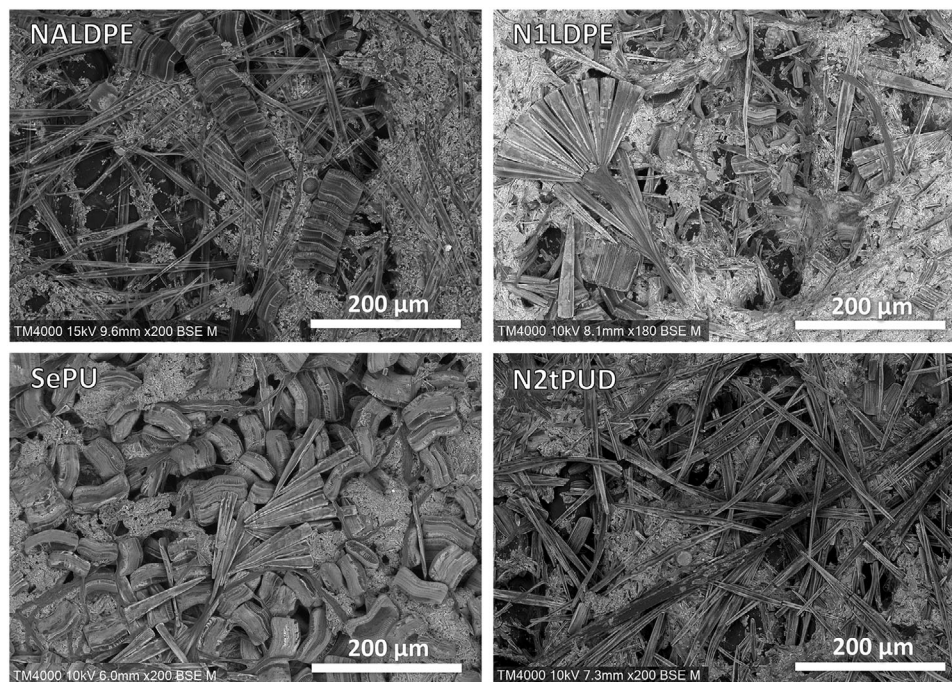


Figure 9. L-V- SEM images of four substrates (NALDPE, N1LDPE, SePU, N2tPUD) randomly picked to highlight the specific diversity of diatom communities encountered in Toulon, in winter (scale bars: 200 µm).

Considering the summer season in Toulon, SePU ($3.1 \cdot 10^4$ cells per μm^2), 44ePU ($2.8 \cdot 10^4$ cells per μm^2), 44HDPE ($2.4 \cdot 10^4$ cells per μm^2) and 44tPUD ($2.6 \cdot 10^4$ cells per μm^2) appear significantly less colonized than SeSi ($6.6 \cdot 10^4$ cells per μm^2) and StPUD ($6.7 \cdot 10^4$ cells per μm^2), which shows the highest densities among all substrates (Figure 8B). Figure 8C shows that 44ePU ($4.2 \cdot 10^{-5}$ μm^3 per μm^2), W1eSi ($4.4 \cdot 10^{-5}$ μm^3 per μm^2), and W1HDPE ($3.6 \cdot 10^{-5}$ μm^3 per μm^2) were significantly less covered in diatom biovolume than SeSi, StPUD, and WAHDPE (all reaching $1.7 \cdot 10^{-4}$ μm^3 per μm^2).

3.4.3. Diatom Alpha and Beta-Diversities

Alpha-diversity analyses was made depending on sites and seasons (Figure 8A,B) and substrates (data not shown) and revealed significant differences between Kristineberg Center and Toulon (Figure S9A, Supporting Information). The observed OTUs and Chao1 index highlighted a higher richness in Toulon ($p < 2.1 \cdot 10^{-13}$) while the probability that two species could be different was higher in Kristineberg Center (see Shannon ($p = 0.004$) and Inverse Simpson ($p = 0.0031$) indexes).

Some LV-SEM images demonstrating the specific diversity of diatom communities encountered in Toulon, in winter can be seen in Figure 9 and in Figure S12 (Supporting Information).

Beta-diversity was analyzed based on the Bray & Curtis index and illustrated on the NMDS (Figure 10B). Whatever the substrate, diatom communities were firstly clustered by the site of immersion (Figure 10A, MANOVA, $p < 0.0001$). Further analyses were performed separately for substrates immersed in Toulon in both seasons and in Kristineberg Center. Results showed that season also significantly affected the communities in Toulon

(MANOVA, $p < 0.0001$). PERMANOVA showed similarity in summer for the microtopography or for the surface chemistry in both sites ($p > 0.05$). In winter in Toulon, pairwise analyses highlighted that only communities on X3 clustered separately (Table S9, Supporting Information).

In Kristineberg Center (Figure 11A), 16 different species were observed with a relative abundance $\geq 5\%$. *Extubocellulus spinifer* was found with a relative abundance ranging from 7 to 30%. For each of the substrates studied, 3 to 7 major species were detected above the threshold of 5%, representing 33 to 62% of all affiliated species. In Toulon, 11 major species were detected with a relative abundance above 5%. *Thalassiosira profunda* was the only one identified on all substrates, varying between 7 and 23% (Figure 11B). *Iconella curvula* did not stand out for all substrates ($< 5\%$ for W1tPUDTS) but reached a maximum of 29% on SHDPETS substrate. Other species (in black) accounted from 14 to 45% depending on the substrate.

LefSe analyses allowed the identification of specific taxa called biomarkers among the communities (Figure 12). Substrates immersed in Kristineberg Center in summer showed in particular the presence of Fragilariales (reaching 14% at best and absent in Toulon) and Cymatosirales classes (relative abundance ranging from 9 to 37% against 1 to 6% in Toulon). The latter was represented almost only by the genus *Extubocellulus* (from 8 to 36%). Naviculaceae family was also specific to Kristineberg Center with relative abundance varying from 7 to 40% (compared to 6% maximum in Toulon), due mostly to the presence of *Navicula ramossissima* (from 3 to 23%) (Figure 12A). In Toulon, in summer, *Sellaphora laevisissima* accounted for 1 to 56% of diatoms identified and explained by itself the consideration of *Sellaphora* and Sellaphoraceae as biomarkers. Similarly, Thalassiosirales, Thalassiosiraceae, *Thalassiosira*, and *Thalassiosira profunda*

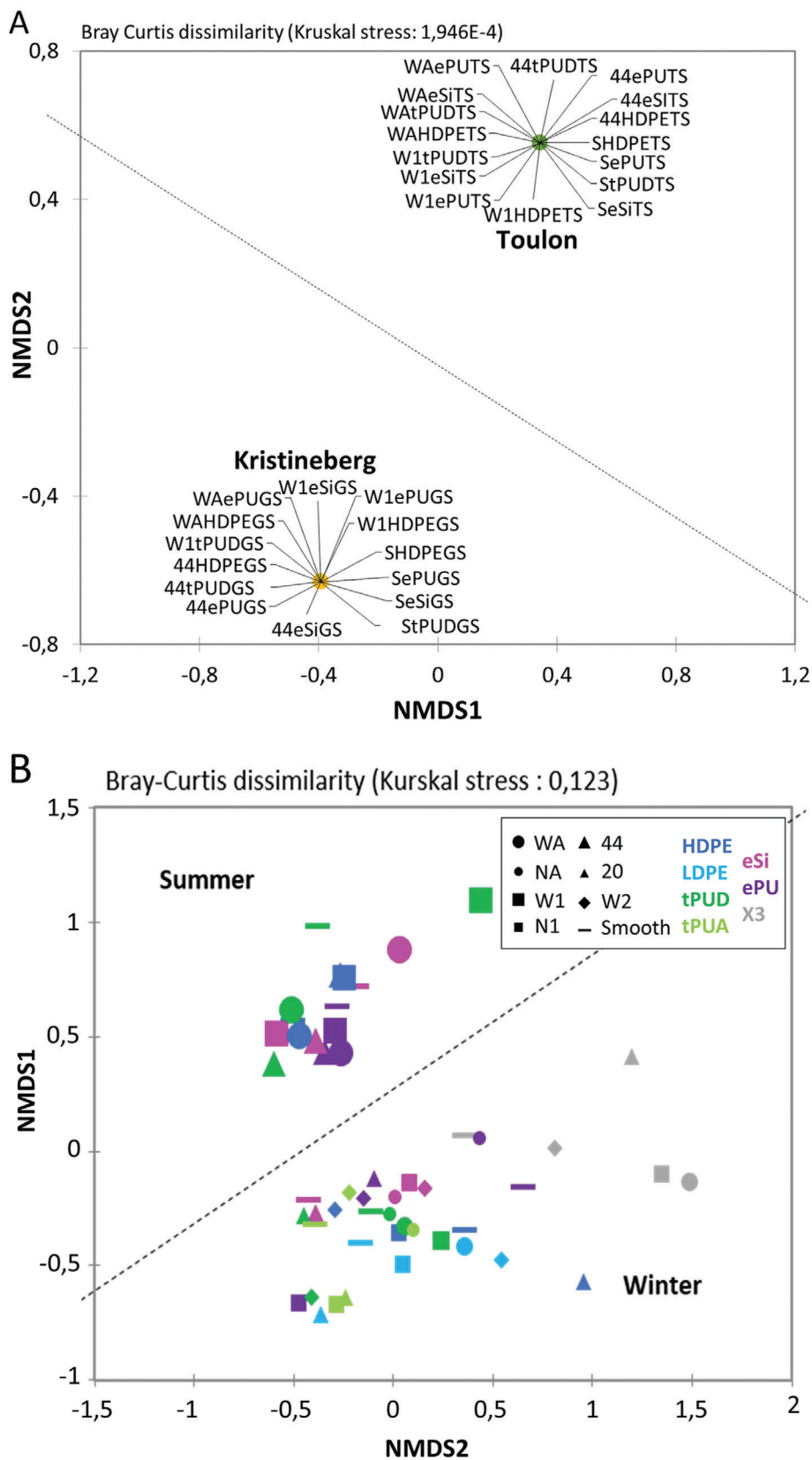


Figure 10. NMDS representation of Bray Curtis dissimilarity between samples, A) according to site immersion and B) season immersion in Toulon. MANOVA p -value was equal to $1E-04$ in both cases. The size of the data points in (B) is related to the number of cells per cm^2 .

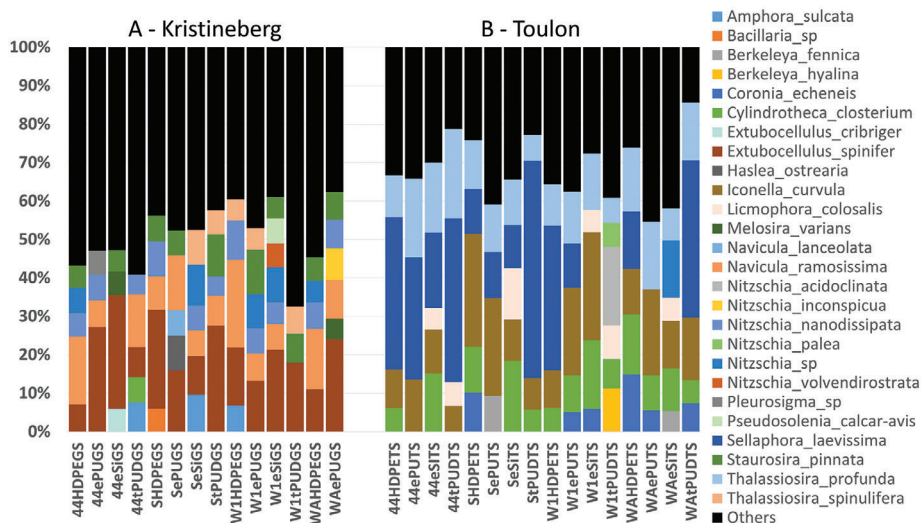


Figure 11. Barplot representation of all diatom species, in relative abundance. Species $\geq 5\%$ are in colors, but species $< 5\%$ are clustered and illustrated in black.

were all considered as biomarkers. Surirellales represented between 5 and 40% in relative abundance at Toulon, compared to a maximum value of 3% at Kristineberg Center (Figure 12A). *Iconella curvula* stood out with 4 to 29% of the readings when *Cylindrotheca closterium* represented 1 to 18% (compared to 7% maximum in Kristineberg Center). When studying seasonal taxa biomarkers in Toulon (Figure 12B), LefSe revealed that most of them were biomarkers for Toulon, either for summer or winter. The latter was also characterized by the slight rise of *Nitzschia* and the clearly specific *Gyrosigma acuminatum* (and its genera), represented at best at 43% when it is only 1% in summer.

4. Discussion

Literature on the effect of physicochemical properties of materials, especially polymers, on the marine colonization process is scarce and partial. Most of the studies used only one biological model, mostly the green algae *Ulva*, and with short immersion times from hours to weeks, which did not integrate kinetics of colonization at the community scale. Conclusions are consequently often limited to predict AF properties on complex marine fouling communities. In this study, we intend to conclusively unravel the effect of microtopographies as well as polymer chemistries, using static field immersion tests at two dissimilar locations in the NW Mediterranean Sea and the Baltic Sea, during both winter and summer at the former, for one month and more. In addition, a multiscale approach was carried out to characterize biofouling communities, including quantitative and qualitative determination of bacterial, diatom and macrofouling assemblages.

4.1. Influence of the Chemistry and Microtopography of Polymer Substrates on Wetting Properties

4.1.1. Effect of Chemistry of Polymers on Wetting Properties

The captive air bubble method was used to be representative to real conditions as the polymer surface is put in contact with arti-

cial seawater. The surface properties are then assessed by depositing a hydrophobic air droplet on the wetted surface. A low $\theta_{\text{air(ASW)}}$ value means that the air bubble does not spread on the surface suggesting that the surface exhibits strong interactions with water molecules, i.e., that the surface has a hydrophilic character.

All the polymers are hydrophilic when immersed in ASW and became more hydrophilic with immersion time (Figure 4). All smooth surfaces were not significantly different when looking at the $\theta_{\text{air(ASW)}}$ values, after 21 days immersed in ASW. tPUA remained the more hydrophobic of the series and ePU remained in the hydrophilic spectrum of the series. HDPE, eSi, and tPUD became significantly as hydrophilic as ePU. It was shown that the water intake over time was low and could not explain this increase of hydrophilicity. The higher mass gain of all polymers due to water absorption was less than 1.8 wt.% after 15 days for ePU (results not shown). The drop in $\theta_{\text{air(ASW)}}$ over the immersion time for tPUA and tPUD surfaces can be explained by the reorientation of urethane functional groups at the surface. The formulation of the commercial tPUA and tPUD is not known, but tPUD should present more urethane functions than tPUA, as it is more rigid (Table 3). This means that tPUD exhibits more hydrogen bonds which led to stronger interactions with water molecules than tPUA when immersed. A $\theta_{\text{air(ASW)}}$ value higher than θ_w for the highly hydrophilic X3 can be explained by the release of the amphiphilic oil from the surface in contact with ASW, resulting in a decrease of its hydrophilicity.^[49] This removal of the excess of amphiphilic oil from the X3 surface in contact with ASW made it difficult to interpret the wetting results. Here the variation between $\theta_{\text{air(ASW)}}$ and $\theta_{w(\text{air})}$ tends to show that the captive air bubble method and the sessile drop method are closer for hydrophobic polymers while for the hydrophilic ones, the difference between the two methods increases. Thus, the surface of hydrophilic polymers changes when they are immersed in a liquid medium, becoming more hydrophilic.

Interestingly, X3 showed a drop of its hydrophilicity once put into water until day 3, from which point the substrate progressively came back to the wetting properties observed at t_0 . The early increase in hydrophilicity of X3 surface during the immer-

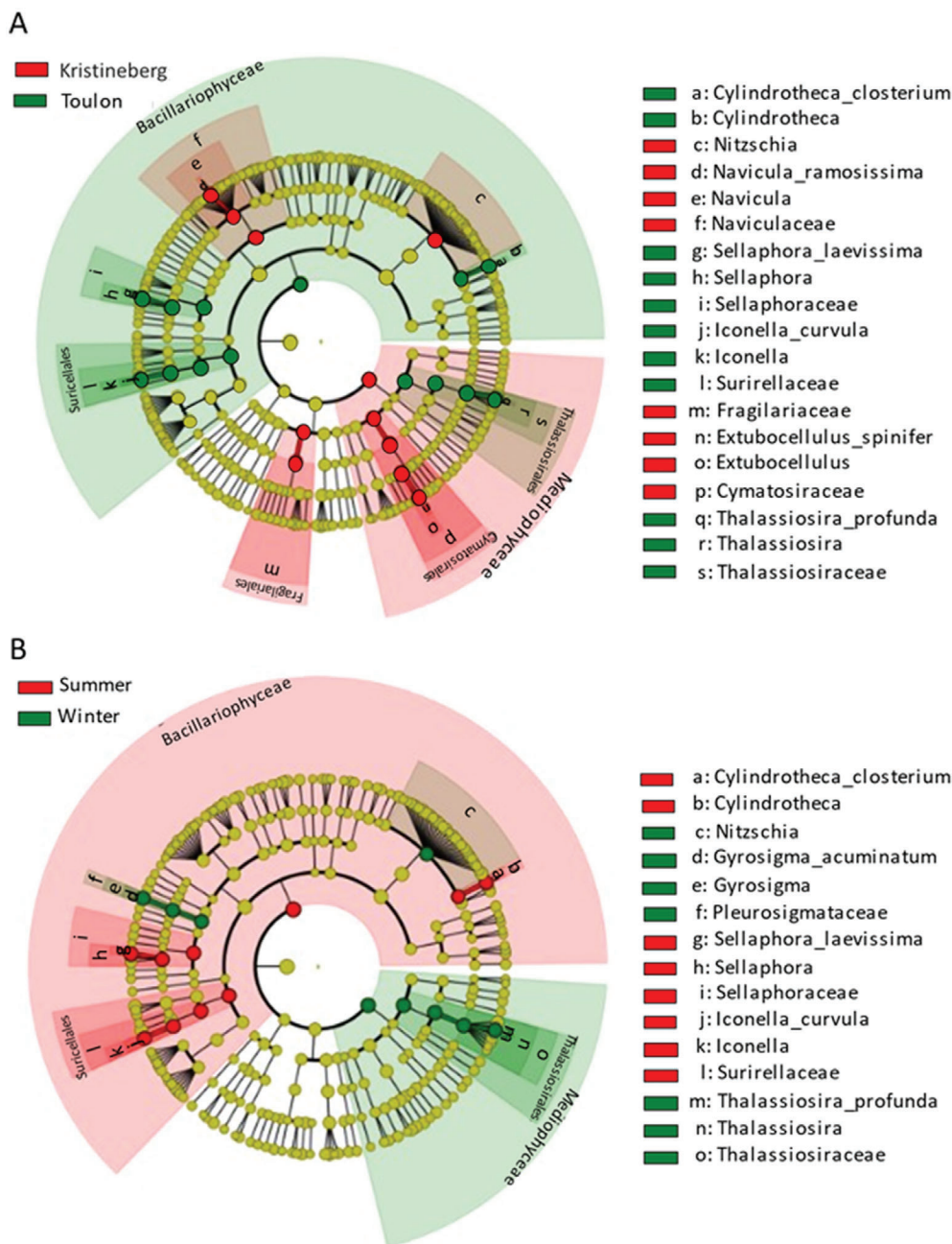


Figure 12. LEfSe analysis cladogram identifying discriminant taxa of diatoms between sites A) or seasons at Toulon B) on all immersed substrates. Taxa with LDA superior to 4.5 are displayed.

sion can come from the diffusion of the amphiphilic additive from the bulk to the surface, leading to an increase of its hydrophilicity with time. Then, the release of this amphiphilic additive in seawater led to an increase of $\theta_{\text{air(ASW)}}$, i.e., an increase of its hydrophobicity before another cycle of amphiphilic oil releasing took place. The experiment lasted only 3 weeks, and the increase of its hydrophobicity back to the initial hydrophobicity after a passage to a more hydrophilic state, was observed at the end of the 3 weeks. Therefore, it cannot be concluded now whether this variation in wetting is something that happens as a cycle, or

whether this variation was observed due to the complete depletion of additive from the bulk. It would have been interesting to see if this mechanism of diffusion could reach an equilibrium up to a complete additive depletion from the substrate or if the diffusion of the additive followed a cycle of variation of the wettability over time of immersion. If the settlement of biofouling on the X3 surface is reduced thanks to a variation of the wetting properties, or by the contact with the additive, it will be possible to conclude whether what was observed here was due to a cycle or a complete depletion of the additive. The release of PEG from

the X3 bulk could perhaps have been verified by measuring the surface tension of the water after prolonged immersion in ASW.

4.1.2. Effect of Microtopography on Wetting Properties

When immersed in ASW, most of the micropatterned polymers exhibited a higher hydrophilic character than the smooth corresponding polymers (Figure 5; Figure S5, Supporting Information). Water seems to fill the features affecting then the spreading of the air bubble. In contrary, micropatterned eSi substrates exhibited a higher $\theta_{\text{air(ASW)}}$ than for the smooth one in immersion leading to a less hydrophilic surfaces than the smooth ones. This result was more pronounced in the \parallel direction than in the \perp direction suggesting that air is entrapped within the features and that the values reflect a hybrid air/eSi surface with a lower fraction of eSi and therefore a higher fraction of air which is more hydrophobic along the length of the features (\parallel direction) than across the features (\perp direction).

Figure 5 also shows that all $\theta_{\text{air(ASW)}}$ values in the \parallel direction for the patterned substrates were higher than $\theta_{\text{air(ASW)}}$ values in the \perp direction, for all polymers and all microtopographies tested. A higher difference between the \perp and \parallel directions was observed for immersed HDPE and tPUD and was higher than the difference between \perp and \parallel directions observed for eSi, ePU, and X3. This last result could indicate that the hardness of the substrates and therefore, the protrusions, could have an impact on the spreading of the air bubble through the microtopography. The difference in wetting behavior was then erased after 3 days of ASW immersion for eSi, ePU, tPUD, and HDPE samples with 44, W1, and WA micropatterning, except X3. Whatever the chemistry of the polymer, the presence of water within the features tends to a similar hydrophilic surface with $\theta_{\text{air(ASW)}}$ around 20–30°. On the contrary, an increase of $\theta_{\text{air(ASW)}}$ values with immersion time was observed for the X3 highly hydrophilic in air which can be explained by the release of the amphiphilic oil from the surface in contact with ASW, as discussed above. The variation in surface properties of micropatterned surfaces has a timescale that should be in phase with the colonization steps of marine fouling when immersed in seawater to limit or inhibit it.

4.2. Effect of the Chemistry and Microtopography of Polymer Substrates on Microfouling and Macrofouling

Surface roughness and micro-(nano-) topographies have been shown to play a role in reducing the settlement of organisms, but only mostly in tests implying one type of organism at a time in laboratory.^[18,19,22] The Baier theory is widely referred to in various publications. The two minima of adhesion described by Baier were settled at a critical surface tension (γ_C) of a substrate between 20 and 30 mN m⁻¹ and between 50 and 70 mN m⁻¹.^[50,51] Here, X3 presents a γ_s value within 50–70 mJ m⁻² and all the other polymers except ePU show a γ_s value within the 20–30 mJ m⁻² range. Therefore, if the Baier theory can apply here, all polymers except ePU should show minimal adhesion.

It would have been interesting to investigate the issue of colonization at an early stage, we chose here to study the microfouling density after 3 weeks of immersion, and all the densities that are

used here, are the densities of biological matter measured after 3 weeks of immersion.

4.2.1. Effect on Microfouling Settlement

Regarding the effect of chemistry, hydrophilic polymers (ePU and X3) seemed to promote the settlement of prokaryote on smooth substrates after the one-month winter immersion with higher densities compared to the other polymers (Figure S8, Supporting Information). All the other polymers did not show significant difference in prokaryote density ($p > 0.05$). In summer, however, smooth ePU substrate's prokaryotic density was found similar to the other smooth substrates in terms of prokaryotic densities. This difference between the communities of organism in Winter and in Summer could explain this result. The X3 substrates were the only ones that showed both a significantly different diatom density and significant difference with other substrates for the prokaryotic density in winter. In summer, the X3 substrates showed a higher density of diatoms, but a smaller biovolume, indicating that smaller diatoms were settled on X3 compared to the other polymers (Figure S10, Supporting Information). In winter, the X3 was significantly different from other substrates with both lower density of diatoms and smaller biovolume (Figure S11, Supporting Information). The lowest values of diatom biovolume of X3 compared to the other substrates in Toulon (in winter and in summer) could be explained by i) a possible distinct composition of the conditioning film (not verified) or ii) a heterogeneous microfouling coverage (see LV-SEM image in Figure S12, Supporting Information) as well as a non-adherent biofilm that hinder the recruitment of larvae and spores.

Regarding the effect of microtopographies and elastic modulus, all the smooth and patterned substrates showed similar prokaryotic densities after the summer immersion. No significant difference with a clear tendency could be noted on the diatom densities between all the patterned and smooth substrates for all polymers except X3. As shown earlier, the influence of the microtopography on the wetting disappeared over time. Since no influence of microtopography could be highlighted, which means that the steric hindrance did not have effect.

Therefore, on a static one-month immersion, neither microtopography, mechanical properties nor “static” chemistry had significant and stable effect on the microfouling settlement.

It was shown elsewhere that, while a difference could be noted between the composition of the bacterial community of various polymers, over a long time of incubation, when exposed to ambient light, the composition of the bacterial community tended to converge with few observable differences.^[52] Shared biofilm core communities were found on various polymers after a long immersion time.^[53] Investigations were made on various polymers immersed for 2 months in 3 sites around Florida in the United States. The colonization of substrates was found similar in each site, and the only difference that was noted was between substrates at different sites, showing the importance of the site on the fouling community. This concurs with the results observed here with few differences between the polymers for a long immersion time. Only biodegradable polymers have been shown to select specific bacterial communities.^[54]

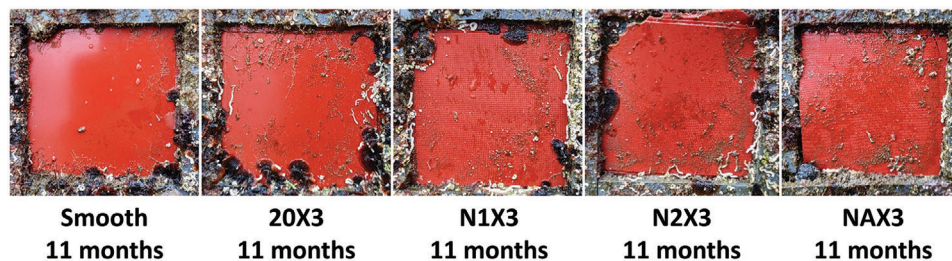


Figure 13. Photographs of smooth and micropatterned X3 substrates (Smooth, 20SK, N1, N2, and NA) after 11 months of immersion in Toulon illustrating that X3 seems to be more efficient against macrofouling when it is smooth rather than when it presents microtopography.

A lot of studies showed a great reduction in settlement thanks to sharklet microtopography, when the dimensions of the Sharklet are adjusted to the size of the targeted microorganism.^[12,18,19,22,55,56] But when the influence of microtopography on fouling settlement was observed, it was mostly (75% of the publications reviewed by Carve and coworkers)^[12] in studies that investigated the settlement of a single organism at a time, without all the complexity that can be found in field tests, and without the presence of biofilm, in a median assay length of 24 h for the publications reviewed by Carve and coworkers. Some studies, however, investigated the AF properties of substrates in field testing (15% of the publication reviewed by Carve and coworkers, with a median maximum duration of 28 days).^[12] Under field conditions, Carve and coworkers reported that textures (various types of microtopographies investigated in their study) were found to have no or inconclusive effect on fouling in most cases (61% of the experiments they reviewed).^[12] For shorter immersion times, Sweat et al. found that diatoms settled better on smooth acrylic panels than on rough acrylic panels when immersed for 2 weeks in the Indian River lagoon.^[57] Here, the substrates were immersed for a long period (1 month) regarding the kinetics of fouling phenomena. The mechanism of adhesion of the two types of microfouling is different as the adhesion of both diatoms and bacteria is related to their production of extracellular polymeric substances (EPS) but bacteria also have external structures such as flagella, fimbriae, curli, and pili that may be involved in their adhesion process.^[58] Further investigations at the molecular level could help to identify the key factors that affect the abundance or the diversity of biofouling on patterned surfaces, such as characterizing the functional groups on the surface and those secreted by the organisms.

4.2.2. Effect on Macrofouling

For the macrofouling, more differences could be noted for the immersion in Kristineberg Center (Figures 6 and 7). The main fouling group observed in Kristineberg Center were *Amphibalanus improvisus* barnacles. Barnacles were reported in several research to prefer high surface energy (30–35 mJ m⁻²).^[59,60] Therefore more barnacles should be observed for tPUD and ePU which presents respective γ_s values of 29 and 44 mJ m⁻². The ePU substrates did show more barnacles than the other substrates with efficacy parameters from 23 to 26 for all the ePU substrates while the other substrates showed an efficacy parameter N below 20 (Figure 7). But tPUD did not appear to recruit more bar-

nacles than the other substrates. Regarding the influence of microtopographies on the settlement of *A. improvisus*, the barnacles seemed to settle following the channels created by the Sharklet (in || the direction) as can be seen in Figure 6.

X3 exhibited the best AF performances in both winter and summer (for the substrates that were not lost). Interestingly, after almost one year in the Mediterranean Sea (from the November 12th, 2019 to October 26th, 2020), when looking at the X3 substrates, the microtopography led to higher N values than the smooth substrate, suggesting that for X3, the microtopography decrease the AF efficacy (Figure 13). Indeed, the X3 is a PDMS elastomer network containing an amphiphilic additive. Its efficacy against fouling could come from its capacity to change its wetting properties over immersion time due to successive steps of migration of additive to the surface (making the substrate more hydrophilic) and wash away of this additive (making the substrate more hydrophobic). It was earlier discussed (in paragraph 4.1.1.) that X3 showed a hydrophilic behavior before immersion due to the oil additive on the surface. Once immersed, the additive was washed off and the static bubble contact angle $\theta_{\text{air(ASW)}}$ measured at t_0 showed that X3 was more hydrophobic. Then over time, some additives migrated to the surface making X3 more hydrophilic again, and this additive was washed off gradually over time of immersion until after 3 weeks, the X3 showed the same hydrophobicity as at t_0 . Figure 13 shows that even after 11 months of immersion, it is likely that the variation of wetting and the release of additive still occurs, implying that it was a cycle that was observed in 4.1.1. and not a complete depletion of the additive from the bulk. Therefore, surfaces with more additive able to migrate to the surface could show more AF efficiency. In Figure 14, the digital images of X3 substrates (smooth, 20, and N) might suggest that more additive is present on smooth substrate. Nevertheless, this quick diffusion of oil during the fabrication steps was not investigated in detail.

The X3 recruited the more diatoms but the biovolume indicated that compared to the other polymers, X3 recruited smaller diatoms, that could fill the spaces between protrusions. Over time, the growth of microorganisms between the protrusions led to the formation of a heterogeneous surface which might cancel the effect of the microtopography. Nevertheless, X3 is still the most efficient substrates against macrofouling over longer time. The recruitment of smaller diatoms does not seem to affect the AF efficacy. The oily and amphiphilic additive at the surface could probably decrease the adhesion strength of biofilms. The AF efficacy was better for NSK microtopographies than for 20SK and that is what is observed after 11 months of immersion with re-

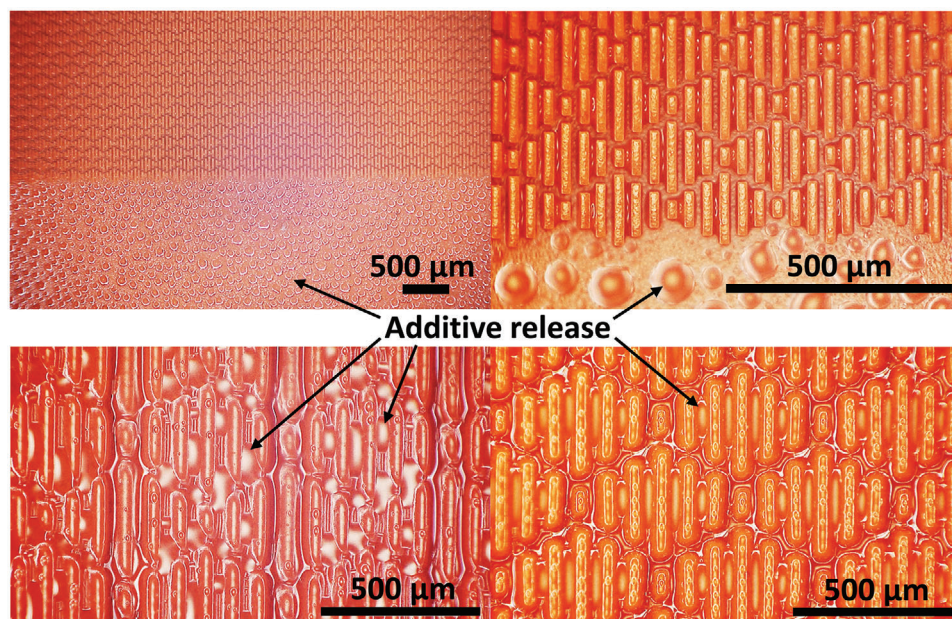


Figure 14. Digital microscopy images of 20×3 (top) and NX3 substrates (bottom). The release of the oily additive creates some droplets on the surface that are more numerous on smooth surfaces (bottom of the 20×3 images) than on micropatterned surfaces. On the microtopography 20×3 , smaller droplets are present between the protrusions than for smooth or for NSK patterned surfaces. On the NSK patterns, the droplets seem more abundant and distributed more randomly on the surface with the less defined protrusions (bottom left) compared to the surface with better-defined features, where the droplet seems to be less numerous and always in the same spots.

spective N efficacy factor of 9 for SX3, 21 for 20X3, 11 for N1X3, 15 for N2X3 and 11 for NAX3.

The result of settlement on X3 substrates, which was minimal for the macroorganisms compared to other substrates, even over one year, showed that it is most likely a cycle of wetting switching that occurs in X3 substrates, and that this mechanism if not totally responsible for the good antifouling properties, at least plays a preponderant role in it.

The effect of chemistry and microtopography can affect the formation of the conditioning film and the settlement of organisms in the early stages of colonization. It may hinder the settlement or the formation of conditioning film at first, but at some point, once the conditioning film was successfully formed, and the pioneer bacteria managed to settle, it will be easier for other organisms to settle and lead to the accumulation of biofilm, and organisms will eventually cover the polymer and/or the microtopography, resulting in a convergence of the fouling for a long time of immersion.

However, X3 showed few to none macrofouling, yet recruiting more bacteria and smaller diatoms than the other polymers. Its variation in wetting, switching gradually from hydrophobic to hydrophilic and from hydrophilic to hydrophobic could have a strong influence on the settlement of fouling. Its low stiffness associated with its changing wetting properties can also result in better fouling release properties and leads to weaker adhesion of the microorganisms and macroorganisms. As its elastic modulus is similar to the one of PDMS (eSi) and ePU polymers, its amphiphilic properties must play an important role in the AF effect of X3 and may help the X3 to not exceed a fouling threshold further which the fouling become not reversible. A hypothesis that can be made is that as X3 becomes very hydrophilic, maybe the accumulation of water interacting with the X3 could lead to

the biofilm stripping off the surface, facilitated by the combined effect of low mechanical property of X3, and the water interaction replacing the bonding of the biofilm to the surface. This would lead to a periodic renewal of the biofilm, which would help hindering the macrofouling settlement. Investigation over time of immersion of the evolution of the biofilm community of the X3 could be of interest to validate or not this hypothesis.

4.3. A RbcI Gene Based Metabarcoding Approach to Study Marine Diatom Diversity

We propose the first metabarcoding approach specifically dedicated to deciphering the diversity of marine diatom communities on artificial substrates in marine environment thanks to the diat.barcode database.^[42] Diatoms or Bacillariophyta are known as the most important contributors to the autotrophic taxa in marine biofilms as they secrete extracellular polymeric substances (EPS), which are involved in the adhesion to substrates.^[61–63] As with bacteria, specific communities adhere to substrates immersed.^[64] Biofilm diatoms were mainly studied using microscopical approach, which is time-consuming and requires a high level of knowledge in morphological identification, especially to reach the species level.^[65–67] They are considered as excellent ecological indicators because of their huge diversity and the fact that particular taxa occupy specific ecological niches. Recently, diatoms were identified with 18S rDNA gene sequencing, which is a non-specific eukaryotic marker.^[64] Unfortunately, this approach failed to identify diatoms to the species level.

The diat.barcode database (previously called R-Syst::diatom) is based on the rbcL (ribulose-1,5-bisphosphate carboxy-

lase/oxygenase large subunit) gene and was developed primarily for freshwater diatoms.^[68,69] Following preliminary studies showing that more than 60% of reads were affiliated with marine or brackish reputed taxa (not shown), we used the diat.barcode database for this study. As expected, around 85% of the taxa were identified to the species level, mostly as marine species. However, one biomarker taxa at Toulon and in the summer, *Iconella curvula*, and spp. in general, were reputed to inhabit freshwater ecosystems (AlgaeBase). In this specific case, the question remains if this taxon, or a close related species, was still not described in marine environments. A huge diversity could be noticed with 551 OTUs in total, representing 165 and 120 species at Toulon and Kristineberg Center, respectively. In conclusion, the curated diat.barcode database constitute a unique opportunity to unravel marine biofilm diatom community drivers, including substrates.

4.4. Influence of the Water Quality and Environment on Fouling Communities

Macrofouling assemblages clearly vary depending on the location and consequently on environmental conditions including the seawater quality.^[70] In this study, both seasons at Toulon and locations significantly influenced macrofoulers. We may consider that the two locations are polluted as they exhibited high human activities but low nutrients and especially phosphates were measured at the Toulon Bay, as in most of the NW Mediterranean Sea. Winter in the NW Mediterranean Sea (Toulon) and summer in the estuary in the North Sea (Kristineberg Center) particularly exhibited a low diversity with mainly brown algae and barnacles, respectively. Previous studies at Toulon allowed to identify low temperature and higher nutrients as main drivers of late autumn-early winter assemblages compared to the more diversified patterns observed in summer.^[71] Nevertheless, the lack of data measured specifically at the Kristineberg Center immersion site failed to determine why only barnacles, generally associated to high temperature and nutrients, colonized substrates in summer.^[72]

Considering diatoms, and similarly to macroorganisms, location induced dissimilar communities, mainly due to differences in water quality.^[73–77] In addition, these articles often reported that environment is a major driver for mature diatom biofilms compared to the nature of substrates, probably in relation with masking effects discussed above. One exception was noticed with biocidal-based antifouling coatings immersed at Toulon and Lorient Bays (Briand et al., 2017). Despite dissimilar environmental conditions, diatom communities were mainly shape by biocides, including a decrease of the alpha diversity, as often reported for bacterial communities.^[78–80] In our study, in line with the literature reported above but despite huge differences in biomass, only the beta diversity was affected by site and seasons. For example, Fragillariaceae (mainly *Staurosira pinnata*) were specific to Kristineberg Center (LEfSe analyses), which appeared consistent with the fact that nutrient favored species with high nutrient tolerances like other species from the same family as *Fragilaria famelica*.^[81] Moreover, one abundant taxa biomarker at Kristineberg Center was the small Mediophyceae *Extubocellus spinifer*, which is representative of the low biomass observed at

the Swedish location but was surprising if high nutrients would be confirmed. As written above for macrofoulers, a more complete characterization of the site would have been necessary to better understand the environmental drivers of the fouling assemblages and why such low richness, diversity, and abundance were observed in the Kristineberg Center. Belando et al. (2017) also observed that metals selected tolerant taxa like *Berkeleya fen-nica*, also identified in our study at Toulon. Metal contamination was notably extensively studied at the Toulon Bay^[82,83] and metal resistance gene quantified in biofilms.^[79] In addition, salinity was reported to promote the genus *Cylindrotheca* to the detriment of *Amphora*,^[76] and this genus was determined as a taxa biomarker at Toulon, which exhibited a higher salinity than the estuarine immersion site in the Kristineberg Center. We also may notice that Chiu and coworkers also observed that community composition in biofilms were affected by salinity in summer while temperature more than salinity shaped winter assemblages, which suggests that additional parameters, including top-down ones like grazing, could interfere.^[76]

5. Conclusion

Among the polymer studied, only smooth and micropatterned X3 samples exhibited the best AF performances against macrofoulers in Toulon. It is worth noting that X3 recruited more bacteria and smaller diatoms in size than the other polymers. As its elastic modulus is similar to the other two PDMS and PU elastomers, its surface properties must play an important role in its AF efficacy over time. Its change in wetting, switching gradually from hydrophobic to hydrophilic and from hydrophilic to hydrophobic with immersion time could have a strong influence on the settlement of macrofouling. Its low stiffness associated with its change in wetting properties may also result in better fouling release properties and lead to weaker adhesion strength of micro- and macro-organisms. This would lead to a periodic renewal of the biofilm, which would help hindering the macrofouling settlement.

The effect of chemistry and microtopography can affect the formation of the conditioning film and the settlement of organisms in the early stages of colonization. It may hinder the settlement or the formation of conditioning film at first, but at some point, once the conditioning film has been successfully formed, and the pioneer bacteria settled, it will be easier for other organisms to settle and the accumulation of biofilm, and organisms will eventually cover the polymer and/or the microtopography, resulting in a convergence of fouling for a long period of immersion.

In addition, it would have been interesting to perform additional fouling release tests on all smooth and micropatterned substrates after short and long immersion time. These tests would have given us more information on i) adhesion, especially using diverse methodologies such as DOPA as a molecular probe, metabolomic or metaproteomic allowing to characterize functional groups, but also the adhesion strength of micro- and macro-organisms on our substrates and ii) its relationship with the water adhesion tension, surface free energy, elastic modulus, and the evolution of wetting properties of the immersed substrates.

Supporting Information

Supporting Information is available from the Wiley Online Library or from the author.

Acknowledgements

E.V. and R.B.-M. contributed equally to this work. Authors thank the IFREMER of La Seyne-sur-mer on the south coast of France and the Kristineberg Center for Marine Research and Innovation on the west coast of Sweden for the access to protected field immersion area. Authors thank the PRECYM (Aix-Marseille Université) for the characterization of the prokaryote densities. Authors also thank the IEMN (Lille, France) for the access to a clean room and the formation to photolithography. This work was supported by the Région SUD- Provence-Alpes- Côte d'Azur (E. V., Ph.D. grant).

Conflict of Interest

The authors declare no conflict of interest.

Data Availability Statement

The data that support the findings of this study are available in the supplementary material of this article.

Keywords

marine biofouling, metabarcoding, microtextured polymers, microtopography, wetting

Received: July 21, 2022

Revised: September 7, 2022

Published online: October 17, 2022

- [1] M. Lejars, A. Margaillan, C. Bressy, *Chem. Rev.* **2012**, *112*, 4347.
- [2] S.-H. Yang, J. W. Ringsberg, E. Johnson, Z. Hu, *Appl. Ocean Res.* **2017**, *65*, 166.
- [3] N. Kip, J. A. Van Veen, *ISME J* **2015**, *9*, 542.
- [4] I. FitrIDGE, T. Dempster, J. Guenther, R. De Nys, *Biofouling* **2012**, *28*, 649.
- [5] P. S. Goh, W. J. Lau, M. H. D. Othman, A. F. Ismail, *Desalination* **2018**, *425*, 130.
- [6] A. M. Brzozowska, S. Maassen, R. G. Z. Rong, P. I. Benke, C.-S. Lim, E. M. Marzinnelli, D. Jańczewski, S. L.-M. Teo, G. J. Vancso, S. L.-M. Teo, G. J. Vancso, *ACS Appl. Mater. Interfaces* **2017**, *9*, 17508.
- [7] F. A. Guardiola, A. Cuesta, J. Meseguer, M. A. Esteban, *Int. J. Mol. Sci.* **2012**, *13*, 1541.
- [8] J. Bannister, M. Sievers, F. Bush, N. Bloecher, *Biofouling* **2019**, *35*, 631.
- [9] P. Hu, Q. Xie, C. Ma, G. Zhang, *Langmuir* **2020**, *36*, 2170.
- [10] A. M. C. Maan, A. H. Hofman, W. M. Vos, M. Kamperman, *Adv. Funct. Mater.* **2020**, *30*, 2000936.
- [11] C. Richards, A. Slaimi, N. E. O'Connor, A. Barrett, S. Kwiatkowska, F. Regan, *Int. J. Mol. Sci.* **2020**, *21*, 5063.
- [12] M. Carve, A. Scardino, J. Shimeta, *Biofouling* **2019**, *35*, 597.
- [13] E. Védie, H. Brisset, J.-F. Briand, C. Bressy, *Adv. Mater. Interfaces* **2021**, *8*, 2100994.
- [14] J. Chapman, C. Hellio, T. Sullivan, R. Brown, S. Russell, E. Kitteringham, L. L. Nor, F. Regan, *Int. Biodeterior. Biodegrad.* **2014**, *86*, 6.
- [15] W. J. Yang, K.-G. Neoh, E.-T. Kang, S. L.-M. Teo, D. Rittschof, *Prog. Polym. Sci.* **2014**, *39*, 1017.
- [16] L. M. Gordon, M. J. Cohen, K. W. MacRenaris, J. D. Pasteris, T. Seda, D. Joester, *Science* **2015**, *347*, 746.
- [17] G. D. Bixler, B. Bhushan, *Nanoscale* **2014**, *6*, 76.
- [18] J. F. Schumacher, M. L. Carman, T. G. Estes, A. W. Feinberg, L. H. Wilson, M. E. Callow, J. A. Callow, J. A. Finlay, A. B. Brennan, *Biofouling* **2007**, *23*, 55.
- [19] J. F. Schumacher, N. Aldred, M. E. Callow, J. A. Finlay, J. A. Callow, A. S. Clare, A. B. Brennan, *Biofouling* **2007**, *23*, 307.
- [20] A. Tripathy, P. Sen, B. Su, W. H. Briscoe, *Adv. Colloid Interface Sci.* **2017**, *248*, 85.
- [21] J. Sun, B. Bhushan, *Tribol. Int.* **2019**, *129*, 67.
- [22] M. L. Carman, T. G. Estes, A. W. Feinberg, J. F. Schumacher, W. Wilkerson, L. H. Wilson, M. E. Callow, J. A. Callow, A. B. Brennan, *Biofouling* **2006**, *22*, 11.
- [23] F. D. Arisoy, K. W. Kolewe, B. Homyak, I. S. Kurtz, J. D. Schiffman, J. J. Watkins, *ACS Appl. Mater. Interfaces* **2018**, *10*, 20055.
- [24] C. J. Long, J. F. Schumacher, A. B. Brennan, *Langmuir* **2009**, *25*, 12982.
- [25] H. Yang, W. Zhang, T. Chen, S. Huang, B. Quan, M. Wang, J. Li, C. Gu, J. Wang, *Molecules* **2019**, *24*, 27.
- [26] X. Xu, A. Awad, P. Robles-Martinez, S. Gaisford, A. Goyanes, A. W. Basit, *J. Controlled Release* **2021**, *329*, 743.
- [27] H. Kadry, S. Wadnap, C. Xu, F. Ahsan, *Eur. J. Pharm. Sci.* **2019**, *135*, 60.
- [28] B. C. Gross, J. L. Erkal, S. Y. Lockwood, C. Chen, D. M. Spence, *Anal. Chem.* **2014**, *86*, 3240.
- [29] C. M. B. Ho, S. H. Ng, K. H. H. Li, Y.-J. Yoon, *Lab Chip* **2015**, *15*, 3627.
- [30] P. J. E. M. V. D. Linden, A. M. Popov, D. Pontoni, *Lab Chip* **2020**, *20*, 4128.
- [31] E. Védie, *Bioinspired engineered-microtopographies for the protection of marine devices against biofouling*, Université de Toulon, **2021**.
- [32] E. Guazzelli, G. Galli, E. Martinelli, A. Margaillan, C. Bressy, *Polymer* **2020**, *186*, 121954.
- [33] C. Coclet, C. Garnier, F. Delpy, D. Jamet, G. Durrieu, C. Le Poupon, M. Mayer, B. Misson, *Prog Oceanogr* **2018**, *163*, 196.
- [34] C. Bressy, J.-F. Briand, C. Compère, K. Réhel, in *Biofouling Methods*, (Eds: S. Dobretsov, J. C. Thomason, D. N. Williams), John Wiley & Sons, Ltd, Weinheim, Germany **2014**, Ch. 12.
- [35] H. Hillebrand, C.-D. Dürselen, D. Kirschtel, U. Pollingher, T. Zohary, *J Physiol* **1999**, *35*, 403.
- [36] M. Camps, A. Barani, G. Gregori, A. Bouchez, B. Le Berre, C. Bressy, Y. Blache, J.-F. Briand, *Appl. Environ. Microbiol.* **2014**, *80*, 4821.
- [37] V. Vasselon, I. Domaizon, F. Rimet, M. Kahlert, A. Bouchez, *Freshw. Sci.* **2017**, *36*, 162.
- [38] F. Escudié, L. Auer, M. Bernard, M. Mariadassou, L. Cauquil, K. Vidal, S. Maman, G. Hernandez-Raquet, S. Combes, G. Pascal, *Bioinformatics* **2018**, *34*, 1287.
- [39] F. Mahé, T. Rognes, C. Quince, C. De Vargas, M. Dunthorn, *PeerJ* **2014**, *2*, e593.
- [40] R. C. Edgar, B. J. Haas, J. C. Clemente, C. Quince, R. Knight, *Bioinformatics* **2011**, *27*, 2194.
- [41] T. Rognes, T. Flouri, B. Nichols, C. Quince, F. Mahé, *PeerJ* **2016**, *4*, e2584.
- [42] F. Rimet, P. Chaumeil, F. Keck, L. Kermarrec, V. Vasselon, M. Kahlert, A. Franc, A. Bouchez, *Database* **2016**, *2016*, baw016.
- [43] N. Segata, J. Izard, L. Waldron, D. Gevers, L. Miropolsky, W. S. Garrett, C. Huttenhower, *Genome Biol.* **2011**, *12*, R60.
- [44] I. O. Ucar, M. D. Doganci, C. E. Cansoy, H. Y. Erbil, I. Avramova, S. Suzer, *Appl. Surf. Sci.* **2011**, *257*, 9587.

- [45] L. Gevaux, M. Lejars, A. Margailan, J.-F. Briand, R. Bunet, C. Bressy, *Polymers* **2019**, *11*, 305.
- [46] M. Dekker, *Handbook of Adhesive Technology*, **2003**.
- [47] F. Azemar, F. Fay, K. Réhel, I. Linossier, *Prog. Org. Coat.* **2020**, *148*, 105841.
- [48] C. Bressy, M. Lejars, *J. Ocean Technol.* **2014**, *9*, 19.
- [49] A. Camós Noguier, S. M. Olsen, S. Hvilsted, S. Kiil, *Prog. Org. Coat.* **2017**, *106*, 77.
- [50] R. E. Baier, E. G. Shafrin, W. A. Zisman, *Science* **1968**, *162*, 1360.
- [51] R. E. Baier, A. E. Meyer, *Biofouling* **1992**, *6*, 165.
- [52] M. Pinto, T. M. Langer, T. Hüffer, T. Hofmann, G. J. Herndl, *PLoS One* **2019**, *14*, e0217165.
- [53] I. V. Kirstein, A. Wichels, G. Krohne, G. Gerdt, *Mar. Environ. Res.* **2018**, *142*, 147.
- [54] C. Dussud, C. Hudec, M. George, P. Fabre, P. Higgs, S. Bruzard, A.-M. Delort, B. Eyheraguibel, A.-L. Meistertzheim, J. Jacquin, J. Cheng, N. Callac, C. Odobel, S. Rabouille, J.-F. Ghiglione, *Front Microbiol* **2018**, *9*, 1571.
- [55] C. A. Kuliasha, J. A. Finlay, S. C. Franco, A. S. Clare, S. J. Stafslien, A. B. Brennan, *Biofouling* **2017**, *33*, 252.
- [56] C. M. Magin, J. A. Finlay, G. Clay, M. E. Callow, J. A. Callow, A. B. Brennan, *Biomacromolecules* **2011**, *12*, 915.
- [57] L. H. Sweat, K. B. Johnson, *Biofouling* **2013**, *29*, 879.
- [58] H. Dang, C. R. Lovell, *Microbiol Mol Biol Rev* **2016**, *80*, 91.
- [59] M. Berglin, P. Gatenholm, *Colloids Surf B Biointerfaces* **2003**, *28*, 107.
- [60] A. Di Fino, L. Petrone, N. Aldred, T. Ederth, B. Liedberg, A. S. Clare, *Biofouling* **2014**, *30*, 143.
- [61] K. E. Cooksey, B. Wigglesworth-Cooksey, *Aquat. Microb. Ecol.* **1995**, *9*, 87.
- [62] M. Salta, J. A. Wharton, Y. Blache, K. R. Stokes, J.-F. Briand, *Environ. Microbiol.* **2013**, *15*, 2879.
- [63] L. A. Amaral-Zettler, E. R. Zettler, T. J. Mincer, *Nat. Rev. Microbiol.* **2020**, *18*, 139.
- [64] S. Oberbeckmann, A. M. Osborn, M. B. Duhaime, *PLoS One* **2016**, *11*, e0159289.
- [65] J. S. Patil, A. C. Anil, *Biofouling* **2005**, *21*, 189.
- [66] J.-F. Briand, A. Barani, C. Garnier, K. Réhel, F. Urvois, C. Lepoupon, A. Bouchez, D. Debroas, C. Bressy, *Microb Ecol* **2017**, *74*, 585.
- [67] K. A. Zargiel, J. S. Coogan, G. W. Swain, *Biofouling* **2011**, *27*, 955.
- [68] V. Vasselon, F. Rimet, K. Tapolczai, A. Bouchez, *Ecol Indic* **2017**, *82*, 1.
- [69] L. Kermarrec, A. Franc, F. Rimet, P. Chaumeil, J.-M. Frigerio, J.-F. Humbert, A. Bouchez, *Freshw Sci* **2014**, *33*, 349.
- [70] S. Dürr, J. C. Thomason, *Biofouling*, John Wiley & Sons, Weinheim, Germany **2009**.
- [71] J.-F. Briand, X. Pochon, S. A. Wood, C. Bressy, C. Garnier, K. Réhel, F. Urvois, G. Culioli, A. Zaiko, *Biofouling* **2018**, *34*, 657.
- [72] G. Courtenay, W. Gladstone, M. Scammell, R. Kidson, J. Wood, *Environ Monit Assess* **2011**, *175*, 685.
- [73] J.-F. Briand, I. Djeridi, D. Jamet, S. Coupé, C. Bressy, M. Molmeret, B. Le Berre, F. Rimet, A. Bouchez, Y. Blache, *Biofouling* **2012**, *28*, 453.
- [74] T. Muthukrishnan, M. Al Khaburi, R. M. M. Abed, *Microb Ecol* **2019**, *78*, 361.
- [75] C. Yang, J. Wang, Y. Yu, S. Liu, C. Xia, *Chin. J. Oceanol. Limnol.* **2015**, *33*, 439.
- [76] J. M. Y. Chiu, V. Thiyagarajan, M. M. Y. Tsoi, P. Y. Qian, *Biofilms* **2005**, *2*, 183.
- [77] S. Mitbavkar, A. C. Anil, *Biofouling* **2008**, *24*, 415.
- [78] T. Muthukrishnan, R. M. M. Abed, S. Dobretsov, B. Kidd, A. A. Finnie, *Biofouling* **2014**, *30*, 1155.
- [79] E. C. P. Catao, N. Gallois, F. Fay, B. Misson, J.-F. Briand, *Environ Pollut* **2021**, *268*, 115835.
- [80] U. Von Ammon, S. A. Wood, O. Laroche, A. Zaiko, L. Tait, S. Lavery, G. Inglis, X. Pochon, *Mar. Environ. Res.* **2018**, *133*, 57.
- [81] M. D. Belando, A. Marín, M. Aboal, A. J. García-Fernández, L. Marín-Guirao, *Sci. Total Environ.* **2017**, *574*, 381.
- [82] C. Coclet, C. Garnier, S. D'Onofrio, G. Durrieu, E. Pasero, C. Le Poupon, D. Omanović, J.-U. Mullot, B. Misson, J.-F. Briand, *Front Microbiol* **2021**, *12*, 292.
- [83] E. Tessier, C. Garnier, J.-U. Mullot, V. Lenoble, M. Arnaud, M. Raynaud, S. Mounier, *Mar. Pollut. Bull.* **2011**, *62*, 2075.